Ann. Rev. Astron. Astrophys. 1980. 18:165–218

THE STRUCTURE OF EXTENDED EXTRAGALACTIC RADIO SOURCES

George Miley
Sterrewacht Leiden, P.O. Box 9513, 2300 RA Leiden, The Netherlands

1 INTRODUCTION

> The very story of the development of the social enterprises of science, technology, economy, and politics throughout the ages does in itself indicate something of the nature of the connections between them.
>
> J. D. Bernal, *Science in History*

The largest, the furthest, the most powerful, and to some of us the most fascinating objects known in the Universe are to be found among the radio sources associated with some elliptical galaxies and QSOs. In recent years it has become apparent that they are also objects of considerable beauty.

This article deals with the appearances of strong extended extragalactic radio sources. Included as "extended" are sources whose sizes are comparable with or larger than a typical galactic diameter, and as "strong," those with intrinsic luminosities at 408 MHz greater than $\sim 10^{23}$ W Hz^{-1}.[1] Compact radio sources have been reviewed recently by Kellermann (1978). Although there are several similarities between the radio properties of the nuclei of spirals and ellipticals (de Bruyn 1978), extended radio emission from spiral galaxies (van der Kruit & Allen 1976) will not be discussed here.

Previous reviews on the structure of extended extragalactic sources have been given by Moffet (1966), Miley (1976), and Willis (1978). Moffet (1975) and De Young (1976) have given more general reviews, the latter

[1]We adopt a Hubble constant of $H = 75$ km s^{-1} Mpc^{-1} throughout and have applied the relevant scaling to all parameters quoted.

0066-4146/80/0915-0165$01.00

emphasizing the theoretical problems involved. Here we concentrate on the observations, stressing the results and literature of the past five years.

Three important types of inference can be attempted from radio source structure. First, the structures, combined with a modicum of imagination, provide clues to the processes that produce the radio sources. Second, with the addition of a large dollop of assumptions, the source structures give information about the physical parameters that characterize the environment of the sources. Third, stretching our credulity and fantasy to the full, source structure can be used to probe the geometry of the Universe. In this article we discuss only the first two. For an account of structure measurements applied to cosmology, see Miley (1976) and Ekers & Miley (1977).

Before considering the present state of our knowledge we review the changes that have taken place in our understanding of the structure of extended radio sources over the last three decades. The main factor in this evolution has been a steady progress in instrumentation and observational techniques. Therefore, although a detailed discussion of instrumental methods (e.g. Cohen 1969) is beyond the scope of this article, a brief summary of the main techniques used for measuring source structure is appropriate. The general properties of commonly observed source morphologies are considered in Section 2. Before dealing with the detailed characteristics of radio components (Section 4), we give an account in Section 3 of how some relevant physical parameters can be derived from the structures. Finally, the relationship of radio-source morphologies to the properties of the parent galaxies and clusters is reviewed in Section 5.

1.1 *Techniques for Measuring Source Structure*

Because of their limited resolution, single dishes are useful only for studying the largest extragalactic sources at short wavelengths. Until recently, owing to receiver instabilities, dynamic ranges greater than 10 to 1 were difficult to achieve. With new observing techniques incorporating multiple beams (Emerson et al. 1979) and cleaning methods (Reich et al. 1978) much larger dynamic ranges have been obtained with the 100-m Effelsberg telescope in Germany.

Several tools have been developed to achieve the higher resolutions needed for studying the structure of extragalactic radio sources. In the technique of interplanetary scintillations, measurements of the degree and time scale of scintillation (flickering) of a source and their variation with distance from the Sun are used to provide useful information on small-scale structure ($<1''$; Hewish et al. 1964, Cohen et al. 1967, Little & Hewish 1968). The scintillation method has the advantage of providing relatively high resolution at low frequencies. However, all but the crudest inferences

about structure depend on the model assumed for the solar wind. Moreover, only sources within a few tens of degrees from the Sun are observed to scintillate and can be studied extensively.

Another way to achieve high resolution is to observe a source as it is occulted by the moon. The variation of flux density then gives its one-dimensional brightness distribution convolved with the diffraction pattern of the moon (Getmansev & Ginzburg 1950, Scheuer 1962, von Hoerner 1964). In contrast to other techniques, the resolution that can be obtained with lunar occultations is not strongly frequency dependent and is mainly governed by signal to noise. A resolution of a few tenths of an arcsecond is readily achievable. There are however three disadvantages of this method. First, it can only be applied to sources that lie on the moon's path. Second, it is difficult to reconstruct the two-dimensional structure without observing several occultations covering a large range of orientations. Third, dynamic ranges of more than 10 to 1 cannot easily be obtained. Despite these limitations the occultation technique has scored two big successes. The occultation of 3C 273 (Hazard et al. 1963) was one of the most crucial observations leading to the discovery of quasars. Also, it was by means of occultation measurements that the relation between the angular sizes and flux densities of radio sources was discovered (Swarup 1975, Kapahi 1975).

By far the most important tool for investigating the structure of radio sources has been interferometry (see Fomalont & Wright 1974 for an excellent account). This uses two or more telescope elements extending over a baseline B to give an angular resolution of λ/B radians. A Michelson two-element interferometer was first applied to astronomy in 1946 by Ryle & Vonberg (1948). Since then the method has undergone many sophisticated developments along two broad fronts.

First, the technique of earth rotational aperture synthesis (Ryle & Hewish 1960) made it possible to produce two-dimensional maps of source structures by Fourier transforming the complex fringe amplitudes using digital computers. The power of aperture synthesis was subsequently increased by the development of restoration methods such as "clean" which removed the distortion in maps due to incomplete sampling of the aperture (Högbom 1974, Schwarz 1978). Several arrays of telescopes linked by cables were built primarily to map the brightness and polarization (Conway & Kronberg 1969, Weiler 1973) distributions of radio sources. Particularly important contributions in delineating radio-source structure on the scale of seconds to minutes of arc have been made by the "One Mile" and "5 km" telescopes at Cambridge, England, the Westerbork telescope in the Netherlands, and NRAO interferometer system at Green Bank, West Virginia. The VLA (Very Large Array) at present being built by the NRAO can attain higher resolution than any of these. Even in its unfinished state

the VLA is now routinely producing maps with resolution of better than 1″ and sensitivity better than 1 mJy.[2]

This resolution is not high enough to probe the range of angular scales within individual sources, which sometimes exceeds 10^6. However, from the beginning of interferometry a second distinct path evolved in which detailed mapping was subordinated to a quest for higher and higher resolution. At Jodrell Bank, England, radio links were used to connect the telescope elements (Brown et al. 1955, Elgaroy et al. 1962). In this way, by 1966 baselines of more than 100 km and resolutions of $\sim 1/20''$ were achieved, at the cost of sacrificing fringe phase information (Palmer et al. 1967). Next, accurate atomic clocks and video tape recorders, which became available during the sixties, were used to develop linkless interferometers. The first examples were completed almost simultaneously in Canada (Broten et al. 1967) and the US (Bare et al. 1967). Very long baseline interferometry (VLBI) with angular resolutions of a fraction of a milliarcsecond could then be carried out. Since the absolute phase of the interferometer fringes cannot yet be generally measured using VLBI, unambiguous Fourier reconstruction of maps is impossible. However, considerable information about fine-scale structure in sources can be extracted by means of the many sophisticated model-fitting schemes now available and from these models a pseudo-map is often produced. The so-called "closure phases," which can be measured with interferometer arrays (Jennison 1958, Readhead & Wilkinson 1978), are particularly valuable in constructing VLBI pseudo-maps.

Aperture-synthesis and VLBI arrays now in operation are listed by Fomalont (1979) and Moffet (1979) respectively.

1.2 *Strategies of Measuring Source Structure*

There are two complementary strategies for obtaining basic information about radio sources from measurements of structure. One can extrapolate conclusions drawn from detailed measurements of individual source morphologies to the whole population of radio sources, or one can try to infer properties of radio sources from statistical analyses of well-defined samples. Highly detailed measurements can only be made for a typical source, e.g. the closest (Cygnus A, Virgo A, Centaurus A) or the largest (3C 236, DA 240, NGC 315, NGC 6251). On the other hand, the statistical approach limits the range of properties one can investigate. And even when samples are chosen with the greatest of care, selection effects that are difficult to take into account often remain.

[2]1 Jansky = 10^{-26} W m^{-2} Hz^{-1} = 10^3 mJy.

1.3 *Source Structure—The Story So Far*

Almost thirty years ago Jennison & Das Gupta (1953) made the fundamental and exciting discovery that Cygnus A, the strongest observed extragalactic radio source, consists of two components which symmetrically straddle the associated optical galaxy and exceed it in size by an order of magnitude. It was gradually established during the next several years that double structure is a very common property of radio sources (Allen et al. 1963, Maltby & Moffet 1963) and that there are often bright regions of emission or "hot spots" within each of the two radio lobes (Allen et al. 1963).

These surprisingly accurate deductions about radio-source structures were made from an analysis of the interferometer fringe amplitudes. Since the mid-sixties earth-rotation aperture synthesis, including fringe-phase data, has been used to map the brightness distributions of several hundred radio sources. The maps confirmed the general features of radio sources that had been extracted from the fringe-amplitude data. Bright hot spots were found frequently at the edges of the intrinsically strongest double sources (e.g. Macdonald et al. 1968, Miley & Wade 1971, Fanaroff & Riley 1974).

Simple models were proposed to explain these observed features. One picture (Burbidge 1967) viewed the extended components as being composed of many thousands of condensed objects each having a mass of $\sim 10^3\ M_\odot$. An alternative model explained the structure of the radio components in terms of evolving plasmons produced in discrete outbursts from the parent nucleus, whose morphologies were governed by interaction with an intergalactic medium (e.g. van der Laan 1963, De Young & Axford 1967, Christiansen 1969, Mills & Sturrock 1970).

An intergalactic medium was also invoked to interpret the more complicated morphologies that were often revealed by detailed radio maps. In particular the tadpole-like "head-tail" radio sources associated with some galaxies in clusters (Ryle & Windram 1968, Hill & Longair 1971) were explained as double sources deformed by the motion of their parent galaxies through an intracluster medium (Miley et al. 1972).

Most of these measurements were made at frequencies of 1400 MHz and below. During the sixties advances in microwave electronics permitted interferometers to be operated at higher frequencies, resulting in the discovery that compact radio cores with relatively flat spectra are frequently embedded in the nuclei of all types of extended radio galaxies and quasars (Dent & Haddock 1965, Barber et al. 1966, Palmer et al. 1967, Mitton 1970). It became clear that the nuclei of these systems frequently remained active for a considerable fraction of the radio-source lifetimes.

These discoveries stimulated the development of models of radio sources in which the lobes are continuously powered by energy channeled or "beamed" quasi-continuously from their nuclei to hot spots in the lobes (Rees 1971, Scheuer 1974, Blandford & Rees 1974, Lovelace 1976, Blandford 1976, Benford 1979, Wiita 1978a,b).

During the past five years considerable progress has been made on the observational front. First there was the discovery that (at least for some nearby radio galaxies) narrow *jets* of radio emission emanate from the nuclear cores and extend far out into the radio lobes (Section 4.4). These jets constituted beautiful circumstantial evidence in favor of beam-type models and probably provide a new way of studying energy transport in radio sources. Second, the detection of *optical emission* has been reported both from some of these radio jets and from radio hot spots in the lobes (Section 4.2). Third, various *alignments* have been demonstrated both within the radio sources themselves and between radio and optical structures (Sections 4.3.3 and 5.2). These imply that the nuclear axis that defines the radio-source phenomenon often stays fixed to within a few degrees during the source lifetime and is fundamentally related to the axis of symmetry of the associated stellar system. Fourth, *multifrequency comparisons* of the total intensity and polarization distributions for several sources have yielded considerable information on the magnetic field distributions and on the physical conditions within the sources and in their environment (Sections 3 and 4).

2 BASIC RADIO SOURCE STRUCTURE

> Not chaos-like, together crushed and bruised,
> But as the world harmoniously confused;
> Where order in variety we see,
> And where all things differ, all agree
>
> Alexander Pope, "Windsor Forest"

2.1 *Commonly Observed Morphologies*

We shall first describe the classes of radio structure that are commonly seen and then show how these morphologies can be ordered in various sequences.

2.1.1 NARROW EDGE-BRIGHTENED DOUBLE SOURCES These sources, which are variously referred to as "classic doubles," "symmetric doubles," "Cygnus A-type doubles," "Type I doubles," and "triples," form the major constituent ($\sim 70\%$) of low frequency radio surveys at high flux levels (3C, 4C, Parkes). They have length-to-width ratios $\gtrsim 4$, and lobes that are brightened at their edges and symmetrically straddle an elliptical galaxy or

QSO. Most radio galaxies with 178-MHz luminosities $\gtrsim 10^{25}$ W Hz^{-1} and most extended radio sources associated with quasars are of this type.

When studied at high resolution ($\gtrsim 5$ pixels across the source) the edge brightening is usually seen to be due to intense compact regions of emission or "hot spots" at the outer edges of the radio lobes. The hot spots have sizes that are typically ~ 1 kpc (Kapahi 1978), i.e. two orders of magnitude smaller than the source as a whole (see Section 2.3). Extended tails or bridges often reach from the hot spots towards the associated galaxy or QSO.

A flat-spectrum radio core is usually associated with the nucleus of the parent galaxy or QSO (see Section 4.3). For this reason these sources are sometimes called "triple." The example shown in Figure 1 is 3C 452 (Högbom 1979).

The overall structure of edge-brightened doubles has several important morphological properties.

(*a*) *Collinearity* As can be seen from Figure 1 the hot spots line up accurately with the nuclear radio core. This is a common property of edge-brightened doubles (e.g. Hargrave & McEllin 1975). In Cygnus A the hot spots and the core are collinear to better than 1° (Miley & Wade 1971, Hargrave & Ryle 1976).

(*b*) *Overall symmetry* The distributions of flux ratios and positional asymmetries between opposite lobes of edge-brightened double sources have been studied at 1.4 GHz (Fomalont 1969, Mackay 1971) and at 5 GHz (Riley & Jenkins 1977, Katgert-Merkelijn et al. 1980, Longair & Riley

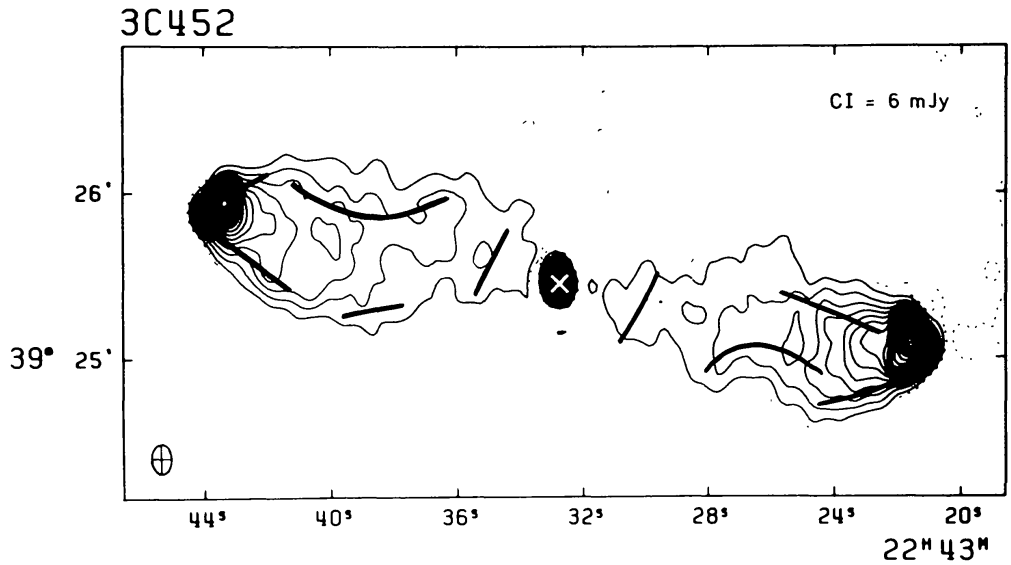

Figure 1 3C 452, a typical narrow edge-brightened double source. Westerbork 5 GHz intensity contour map with magnetic field directions superimposed. The cross indicates the position of the nucleus of the associated galaxy (from Högbom 1979 and kindly supplied by the author).

1979). The reader should be cautious in reading too much into the detailed statistics because the likelihood of an optical identification is biased in favor of symmetric sources. It is clear, however, that components of limb-brightened doubles are quite similar. The strongest component is observed to be more than twice as strong as the weaker one in only about 30% of the sources. The components are also usually symmetrically distributed with respect to their parent nuclei; the distances to opposite extremities rarely differ by more than 50%. Components of sources associated with quasars tend to have less similar flux ratios and to be more asymmetric than those associated with galaxies. For the radio galaxies the components closest to the nuclei tend to be the brightest, but this trend is not apparent in the case of the quasars.

In some sources (e.g. 3C 273; Conway & Stannard 1975), extended structure is seen only on one side of the nucleus, the flux ratio between opposite lobes usually exceeding 10:1. These highly asymmetric sources are sometimes called "D2 doubles" (Miley 1971, Conway & Stannard 1975, Davis et al. 1977, 1978) or "C-sources" (Readhead et al. 1978a). It is not clear whether these sources are members of a different species or whether they represent the tail of a continuous distribution of relative brightness. Three of them have recently been mapped with the VLA (Perley & Johnston 1979). Such sources make up $\sim 10\%$ of all extended quasars (Stannard & Neal 1977, Miley & Hartsuijker 1978). One-sided sources identified with galaxies are rarer but are still occasionally seen (e.g. Argue et al. 1978). Apparent differences between radio galaxies and quasars may merely reflect a dependence on luminosity, since the more luminous sources are almost all quasars; see Section 5.2.

(*c*) *Alignment* The agreement between the orientation of the cores and that of the overall structure of symmetric edge-brightened doubles is discussed in Section 4.3.3. Alignment on an intermediate scale is seen in the bridges that extend from the hot spots to the cores and in which enhancements are sometimes present (e.g. Goss et al. 1977).

2.1.2 NARROW EDGE-DARKENED DOUBLE SOURCES Several narrow double sources have brightness distributions that gradually die away at their extremities. The closest radio galaxy Centaurus A (Cooper et al. 1965) falls into this class. Figure 2 shows 3C 449, another good example (Perley et al. 1979, Bystedt & Högbom 1979). 3C 31 (Burch 1977b) and the two radio galaxies that make up 3C 402 (Riley & Pooley 1975) are also of this type.

These radio sources usually have radio cores (Section 4.3). When studied with high enough resolution, narrow collimated radio jets are often seen to emanate from their nuclei (Section 4.4). They are sometimes called "3C 31-types" (Simon 1978).

2.1.3 WIDE DOUBLE SOURCES A few relatively relaxed doubles have fatter lobes with length-to-width ratios of 2 or 3. Figure 3 shows 3C 310 (van Breugel 1980a). Other examples are Virgo A (Andernach et al. 1979), Fornax A (Cameron 1971), Centaurus A (Cooper et al. 1965), and 3C 314.1 (Miley & van der Laan 1973).

2.1.4 NARROW TAILED SOURCES These have a tadpole-like asymmetric structure, with a high brightness head that coincides with the nucleus of an elliptical galaxy and a diffuse tail that often extends for several hundred kpc. Alternative names by which this species is known are "head tail" or "narrow angle tail" (NAT) source. In some cases their morphology is observed to be two-pronged with a double tail and/or a double head. The ability to distinguish between "twin tailed" and "single tail" sources sometimes depends on the resolution and dynamic range of the observations.

Shown in Figure 4 is 3C 83.1B/NGC 1265 (twin) and in Figure 6 IC 310 (single), both radio galaxies in the Perseus Cluster. Other examples of narrow twin-tailed sources are 3C 129 (Miley 1973), B2 1108 + 41 (Rudnick & Owen 1977, Valentijn 1979a), B2 1502 + 28 (Valentijn 1979a), and 4C 39.49 (Miley & Harris 1977).

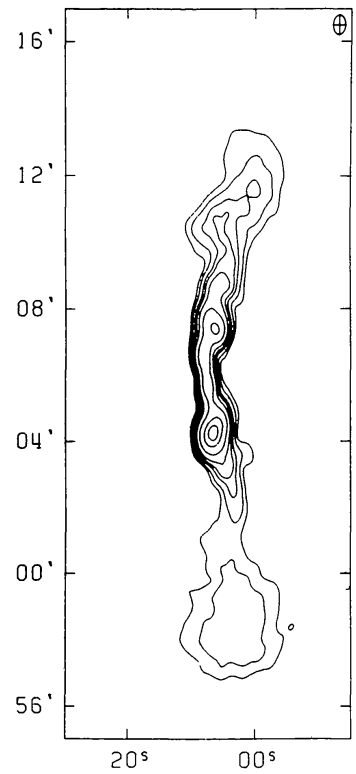

Figure 2 3C 449, a narrow edge-darkened double source. Westerbork 1.4 GHz intensity contour map (from J. Bystedt and J. A. Högbom, in preparation, and kindly supplied by the authors).

Radio cores are usually found in tailed sources (see Section 4.3). When studied with sufficiently high resolution the heads are often resolved into narrow jets of radio emission (see Section 4.4).

2.1.5 WIDE-TAILED SOURCES The structure of these sources is intermediate between that of the narrow edge-darkened doubles and the narrow twin-tailed sources. A common alias by which they are known is "WAT" (wide-angle tail). Shown here, in Figure 5, is 3C 465 (van Breugel 1980c). Other examples are IC 708 (Vallée & Wilson 1976, Wilson & Vallée 1977, Vallée et

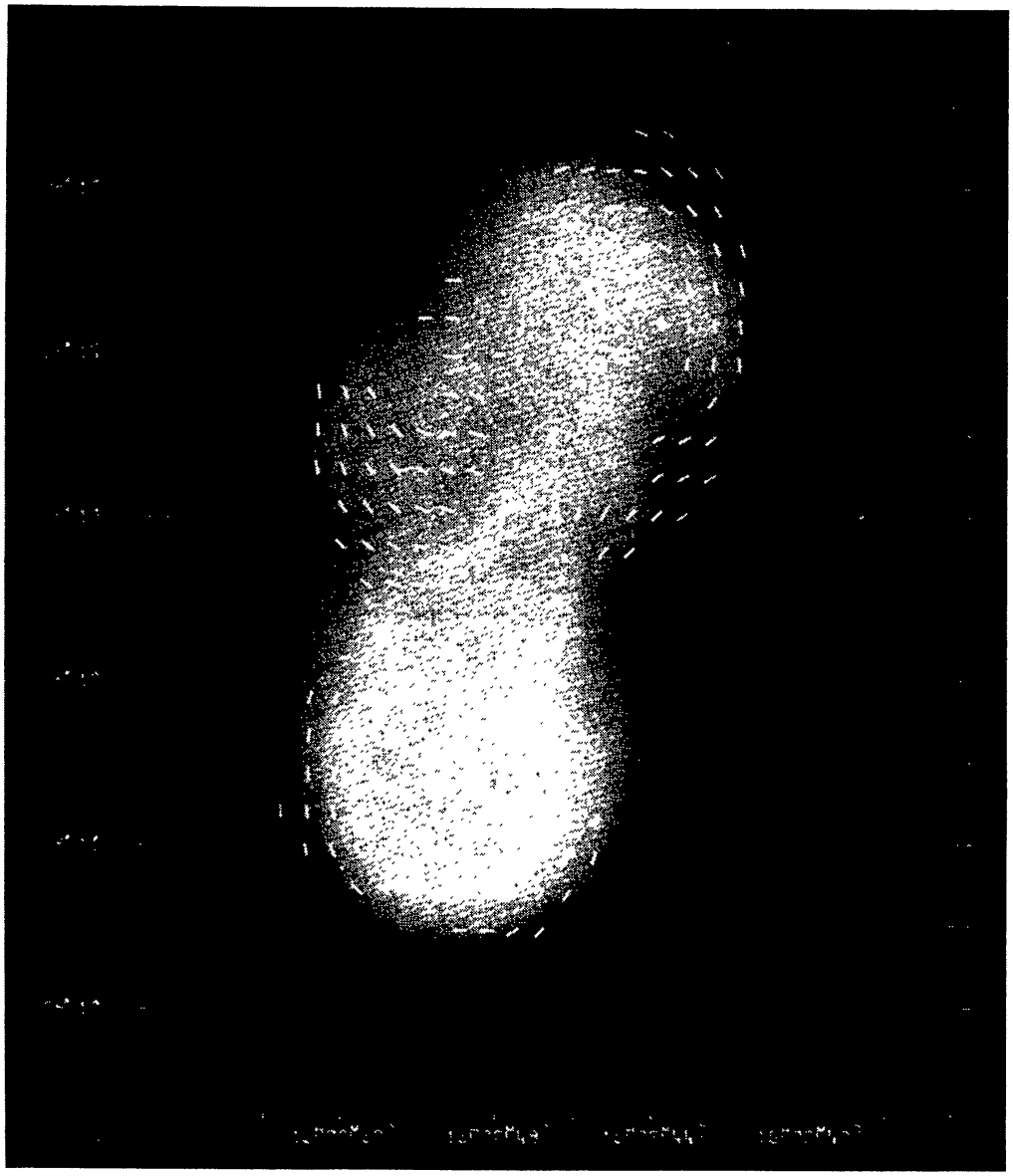

Figure 3 3C 310, a wide double source. Radiophoto of the total intensity distribution (Westerbork 5 GHz) with magnetic field directions superimposed (from van Breugel 1980a and kindly supplied by the author).

al. 1979), B2 0658+33B, B2 0836+29, and B2 0838+32A (Valentijn 1979a), NGC 6034 (Valentijn & Perola 1978), and 4C 48.21 (Owen & Rudnick 1976).

2.1.6 CLUSTER HALOS Several clusters of galaxies have associated large radio components with steep nonthermal spectra ($\alpha \lesssim -1.2$) which often

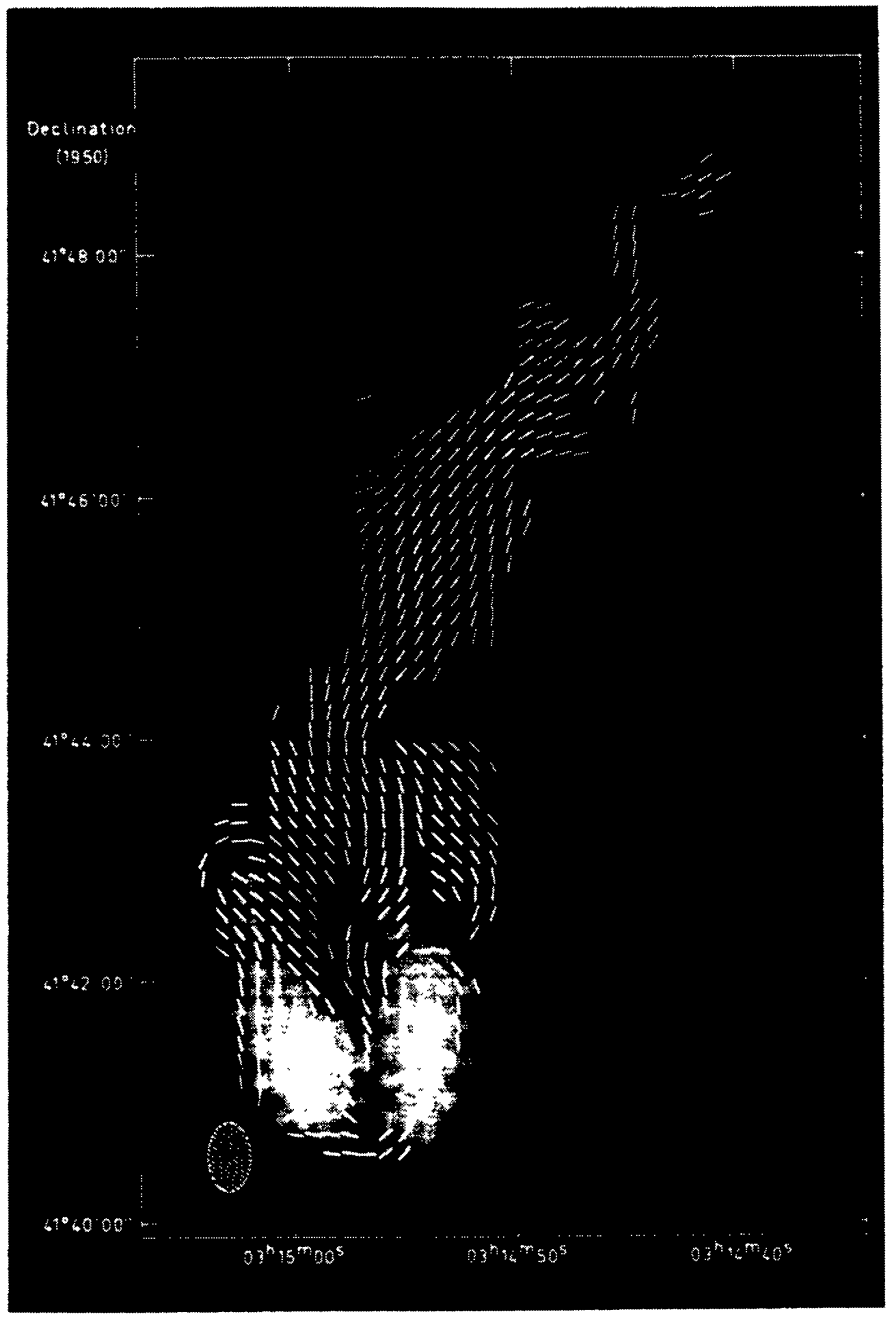

Figure 4 3C 83.1B/NGC 1265, a twin-tailed source in the Perseus Cluster. Radiophoto of the total intensity distribution (Westerbork, 1.4 GHz) with magnetic field directions superimposed (from Miley et al. 1975).

dominate the cluster radio emission at frequencies below 100 MHz (e.g. Baldwin & Scott 1973, Slingo 1974). Instruments operating at this low frequency have insufficient resolution to map them and they are extremely difficult to detect at high frequencies owing to their faintness and confusion from other sources in the cluster. Therefore little is known about them. The sources of this class to have been studied in most detail are Coma C, a smooth diffuse halo in the Coma Cluster with a size of $\sim 40'$ (1.2 Mpc; Jaffe et al. 1976, Jaffe 1977, Valentijn 1978, Hanisch et al. 1979) and Abell 2256 where the situation is complicated (Bridle & Fomalont 1976, Masson & Mayer 1978, Bridle et al. 1979b). Other possible examples are in Abell 1367 (Gavazzi 1978) and Abell 2139 (Harris & Miley 1978), but the cluster halo 3C 84 B reported to be in the Perseus Cluster (Ryle & Windram 1968) has been shown to be nonexistent (Gisler & Miley 1979, Birkinshaw 1980, Jaffe & Rudnick 1979).

It has been suggested that cluster halos are the remnants of tailed radio

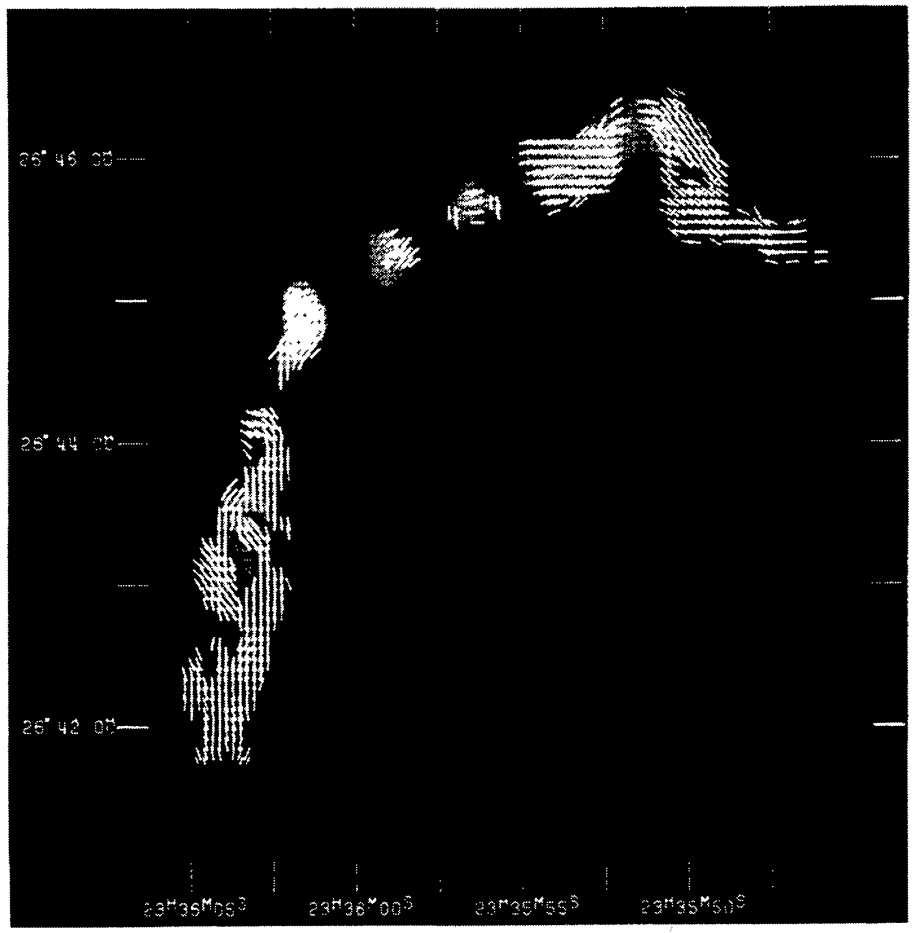

Figure 5 3C 465/NGC 7720, a wide-angle tailed source. Radiophoto of the total intensity distribution with magnetic field directions superimposed (from van Breugel 1980c and kindly supplied by the author).

galaxies whose spectra are steepened by synchrotron losses (e.g. Harris & Miley 1978) or interfaces between two subclusters undergoing coalescence (Harris et al. 1980).

2.2 *Taxonomy of Extended Sources*

The taxonomic approach to radio morphology attempts to recognize recurrent patterns that could give useful phenomenological information about the mechanisms involved. Pattern recognition depends on the amount of detail delineated by a given observation, i.e. both on the number of pixels (beam elements) across the source and on the dynamic range in brightness that can be studied.

Bearing these remarks in mind we now consider some similarities and differences between the various types of radio sources described in Section 2.1. The duplicity of the large-scale structure, the widespread presence of radio cores, and the nuclear collimation in wide sources (see Section 4.3) all suggest that the mechanisms for producing the radio sources are similar and occur in the parent galaxy nuclei.

However, as we have seen, there are also several differences. Three gross structural properties have emerged as being particularly important in studying these morphological differences. In order of the increasing amount of relative detail needed to discern them they are 1. the overall bending at the outer extremities, 2. the edge-brightening, 3. rotational symmetry. These properties define three sequences along which the large-scale structure of almost all sources can be classified, allowing for projection effects.

2.2.1 BENDING SEQUENCE—RADIO TRAILS The bending sequence is illustrated in Figure 6. The simplest measure of source bending is the angle subtended at the radio core or nucleus by lines drawn to the extremities of opposite lobes. An analysis of the distribution of this "opening angle," χ, for a sample of 44 tailed and double sources has been given by Valentijn (1979b). Opening angles between 0° (narrow-tailed source) and 180° (double source) are seen, with a possible small zone of avoidance $45° < \chi < 90°$. The bending sequence extends fairly continuously from double sources to narrow tailed sources, so any discussion of bending that includes only double sources (Harris 1974, Ingham & Morrison 1975) seems unnecessarily restrictive. The opening angle seems to be correlated with the absolute magnitude of the parent galaxy; narrow tails are associated with fainter galaxies than the wider tails (Rudnick & Owen 1977, McHardy 1979, Simon 1978, Valentijn 1979b). The bending is most simply explained as distortion of an initially collimated double morphology by translational motion with respect to a surrounding intergalactic medium (Miley et al. 1972).

Within this picture, therefore, tailed sources are viewed as trails or fossil records deposited by active galaxies. This interpretation is supported by (*a*) similarities between the fine-scale structure of tailed and double sources (Section 4.4; Miley 1974) and (*b*) the preferential occurrence of the most bent sources in dynamically active clusters containing hot gas (Section 5.4). A number of radio-trail models have been proposed to account for the detailed brightness and polarization distributions (e.g. Jaffe & Perola 1973, Pacholczyk & Scott 1976, Cowie & McKee 1975, Jones & Owen 1979).

2.2.2 EDGE-BRIGHTENING SEQUENCE—MORPHOLOGY AND LUMINOSITY The edge-brightening sequence is illustrated in Figure 7. There is a striking correlation between the degree of edge brightness of a source and its luminosity. This was first noted by Fanaroff & Riley (1974) who examined the structure of 3C sources as a function of luminosity at 178 MHz (P_{178}). For $P_{178} \lesssim 10^{26}$ W Hz^{-1} ("Class I") almost all sources have a relatively relaxed morphology, while for $P_{178} \gtrsim 10^{26}$ W Hz^{-1} ("Class II") almost all are edge-brightened doubles.

This critical luminosity is tantalizingly close to the break in the radio luminosity function for elliptical galaxies, which, scaling from Auriemma et al. (1977), occurs at $\sim 1.9 \times 10^{25}$ W Hz^{-1}. The break in the luminosity function separates sources that show strong population evolution (the more luminous sources) from those that do not.

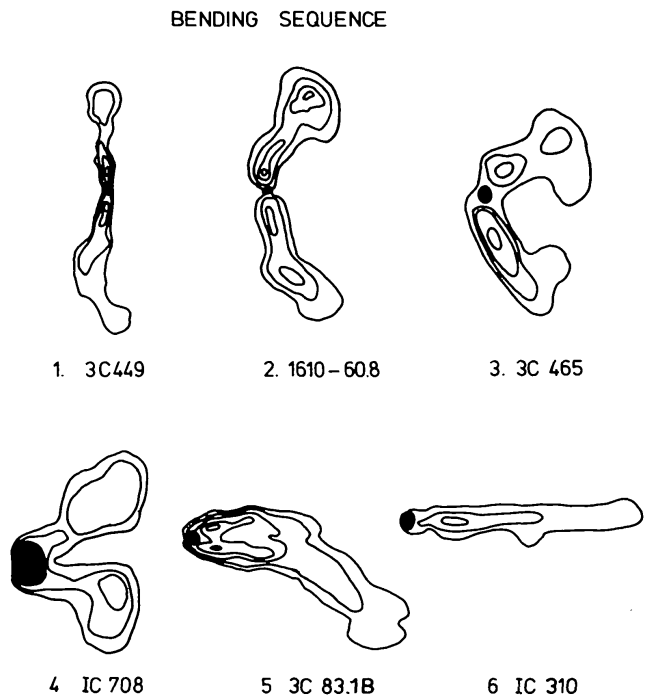

Figure 6 A sequence of radio-source bending illustrated with schematic drawings of actual sources.

Further work (Jenkins & McEllin 1977, Speed & Warwick 1978) suggested that for the edge-brightened doubles themselves the fractional flux in the hot spots increases with luminosity. However, Kapahi has pointed out that this might be caused by selection. Owing to the limited resolution on the maps of the strong sources, linear size evolution of the hot spots might cause the more distant (stronger) ones to appear more intense.

The lower luminosity (Class I) sources are a mixed bag. They include wide doubles, edge-darkened doubles, tailed, and complex sources. There are indications that the degree of bending (the opening angle in the bending sequence) decreases with luminosity, the wide-angle tails being more luminous than the narrow-angle tails (Owen & Rudnick 1976, Simon 1978, Valentijn 1979b). This can be qualitatively understood: One would expect outbursts in the more powerful sources to involve more kinetic energy, and the distorting pressure of an intergalactic medium on their evolution to be consequently smaller. Alternatively, the lower luminosity sources are presumably associated with less massive galaxies which may on average be moving faster.

2.2.3 ROTATIONAL SYMMETRY Also shown in Figure 7 are some examples of two-dimensional rotational symmetry (S or Z shape) which is seen in

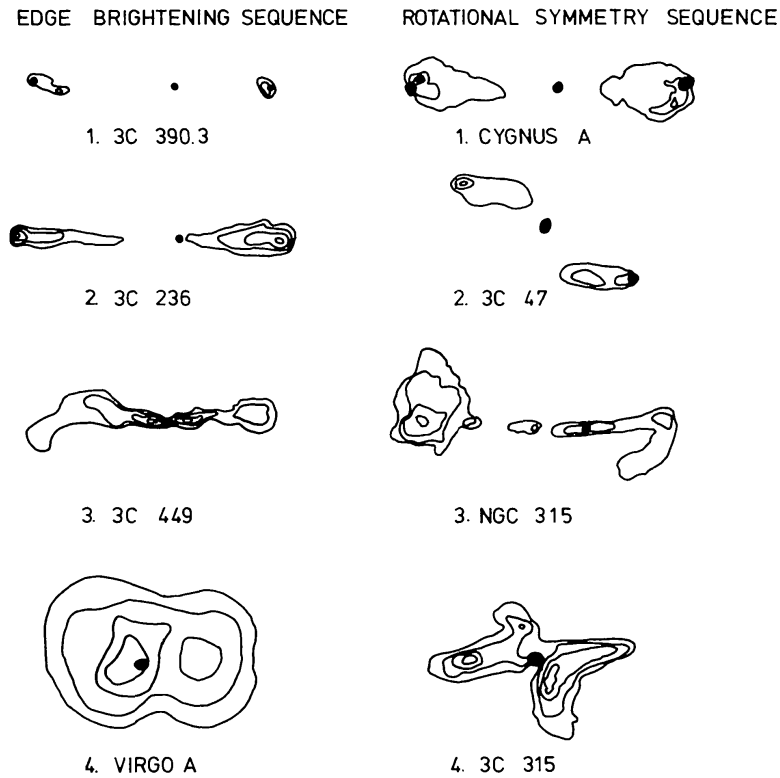

Figure 7 Sequences of edge-brightness and rotational symmetry illustrated with schematic drawings of actual sources.

many radio sources (Harris 1974, Miley 1976). This symmetry was first observed in Centaurus A (Cooper et al. 1965) and is particularly evident in 3C 47 (Pooley & Henbest 1974, Miley & Hartsuijker 1978), 3C 272.1 (Jenkins et al. 1977), NGC 315 (Bridle et al. 1976, Bridle et al. 1979a), and the outer components of Cygnus A (Hargrave & Ryle 1974). A possible cause is distortion of the structure by rotation or shear in the intergalactic medium. But to explain the Z shapes in giant sources such as NGC 315 such motions must take place over scales of more than a megaparsec. An alternative hypothesis is a swinging of the fundamental nuclear ejection axis during the lifetime of the source (Miley 1976). The symmetries in 3C 315 (Northover 1976, Högbom 1979) and B2 0055+26/4C 26.03/NGC 326/(Ekers et al. 1978a) are indeed suggestive of precessing nuclear beams. A scenario in which such precession could occur was sketched by Rees (1978b). Misalignment between the rotational axis of the nuclear machine (a black hole) and the angular momentum axis of the galaxy is supposed to take place as a result of galaxy merging. It is noteworthy that both 3C 315 and B2 0055+26 are associated with close pairs of galaxies. Precession could also occur as the central black hole was accreting material from a cloud or disk with a different angular momentum direction from that of the galaxy as a whole. See Section 5.3.

2.3 *Overall Linear Sizes of Sources*

The linear sizes of extended extragalactic sources span on enormous range, from sources like 3C 346 (Pooley & Henbest 1974) which are no larger than their parent galaxies to giant sources like 3C 236 with a total size in its largest direction of 4 Mpc (Willis et al. 1974, Strom & Willis 1979). The size distribution and its dependence on source structure and luminosity have been considered by Gavazzi & Perola (1978) using well-defined 3C and B2 samples. To minimize cosmological effects and ensure completeness they restricted their study to (104) elliptical galaxies with $z < 0.1$. Unfortunately, this inevitably excluded the highest luminosity sources, which tend to be the most distant. The luminosities considered ranged from $P_{178} \sim 10^{23.4}$ to $\sim 10^{27}$ W Hz^{-1}.

The sizes of edge-brightened doubles are well defined. The linear size function for these sources indicates a slight increase of size with luminosity ($\propto P^{1.4}$), with a median value of ~ 170 kpc at 10^{25} W Hz^{-1}. Most have sizes between 150 and 300 kpc with a few ($\lesssim 5\%$) that exceed a megaparsec. Only 10% of the two-sided edge-brightened sources are smaller than 130 kpc, suggesting that either the outward motion of source components decelerates rapidly after reaching this size or that the smaller sources are effectively invisible. The one-sided sources (Section 2.1.1) appear to be

smaller than the symmetric ones, with typical sizes of a few tens of kpc (Readhead et al. 1978a).

The situation for the more diffuse (Class I) sources is unclear. The median size (~ 150 kpc) of the relaxed doubles and the sizes of their largest members are comparable with those of the edge-brightened doubles. In the data of Gavazzi & Perola there is no significant dependence of the total linear size on luminosity for the diffuse sources, but the uncertainties are large. Because of their ill-defined extremities, estimates of the total sizes of the Class I sources are affected by the sensitivity of measurement. However, sometimes the diffuse sources have regions of enhanced emission *within* their lobes and the separation of these hot spots provides a less subjective yardstick than the total linear extent of the source. The linear distance of those hot spots from their parent nuclei seems to increase with source luminosity (Birkinshaw et al. 1978). In view of the similar results for sources of diverse morphologies the increase in separation of the hot spots with the total source luminosity is quite well established. Such an effect would be intuitively expected, for example, if the more powerful sources are associated with more powerful nuclear ejecta or beams which can penetrate further into the surrounding medium.

It should be stressed that great caution should be exercised in interpreting linear size functions since the results often depend on whether the function is plotted linearly or logarithmically (Ekers & Miley 1977).

3 PHYSICAL PARAMETERS

> In the early treatizes on this subject, the mean value assigned to π will be found to be 40.000000. Later writers suspected that the decimal point had been accidentally shifted, and that the proper value was 400.00000.
>
> Lewis Carroll, "The new method of evaluation as applied to π," from *Notes by an Oxford Chiel*

Total intensity and polarization data can be used to extract information about several physical parameters intrinsic to radio sources and thereby help place constraints on some of the mechanisms involved. Since the advent of computers and more recently of pocket calculators, this "interpretation of the data" has become such an automatic ritual that the many assumptions inherent in each step are sometimes forgotten. We shall review here some of the arguments most commonly used in deriving physical parameters from intensity and polarized brightness distributions. In order to make the uncertainties more explicit, the formulas will be expressed as much as possible in terms of observed quantities. For block

diagrams of the various steps and assumptions that are made the reader is referred to Miley (1976).

3.1 *Total Intensity Distributions*

3.1.1 ENERGETICS The energetics of radio sources are important not only because of their relation to the source-production mechanism but because they also play an important role in all considerations of how radio sources are held together or confined. Total intensity distributions provide information about the minimum energies involved. A good discussion of source energetics is given by Moffet (1975) and in more detail by Pacholcyzk (1970). The minimum energy condition corresponds almost (but not quite) to equipartition of energy between relativistic particles and magnetic field.

For a region in a synchrotron radio source delineated by an ellipse of angular diameters θ_x and θ_y in orthogonal directions, we can write the minimum energy density as

$$u_{me} = (7/3)(B_{me}^2/8\pi) = 0.0928\, B_{me}^2 \text{ erg cm}^{-3} \tag{1}$$

where the corresponding magnetic field is

$$B_{me} = 5.69 \times 10^{-5} \left[\frac{(1+k)}{\eta} (1+z)^{3-\alpha} \frac{1}{\theta_x \theta_y s \sin^{3/2}\phi} \times \frac{F_0}{\nu_0^{\alpha}} \frac{\nu_2^{\alpha+1/2} - \nu_1^{\alpha+1/2}}{\alpha+\frac{1}{2}} \right]^{2/7} \text{gauss.} \tag{2}$$

Here k is the ratio of energy in the heavy particles to that in the electrons, η is the filling factor of the emitting regions, z is the redshift, θ_x and θ_y (arcsec) correspond either to the source/component sizes or to the equivalent beam widths, s (kiloparsec) is the path length through the source in the line of sight, ϕ is the angle between the uniform magnetic field and the line of sight, F_0 (Jy or Jy per beam) is the flux density or brightness of the region at frequency ν_0 (GHz), ν_1 and ν_2 (GHz) are the upper and lower cut off frequencies presumed for the radio spectrum, and α is the spectral index $[F(\nu) \propto \nu^{\alpha}, \nu_1 < \nu < \nu_2]$.

Apart from the basic assumptions that the radiation is synchrotron emission and that the radio and optical emission are redshifted by the same amount there are several more mundane uncertainties inherent in these formulas.

First, k is unknown and could have a value between 1 and 2000 (Pacholczyk 1970). Indirect arguments have usually led to canonical values of $k = 1$ or $k = 100$ (eg. Moffet 1975). $k = 1$ is clearly more consistent with the use of the minimum energy condition. Note that a difference of 100 in

the assumed k results in an order-of-magnitude difference in the minimum energy densities derived. Second, to obtain s, the path through the source along the line of sight, one must make some assumptions about the symmetry and distance of the source. Frequently cylindrical symmetry is assumed, with s equal to the width of the source in the plane of the sky. Third, the formulas depend on the form of the source spectrum, but this dependence is weak. For extended sources $\alpha \lesssim -0.6$, and ν_1 dominates over ν_2. Usually $\nu_1 = 0.01$ GHz is assumed. Fourth, the $\sin\phi$ term is unknown in individual cases. It arises because the emission measure depends on the perpendicular component of the magnetic field and the visible radiation is beamed from electrons moving towards us. Fifth, and perhaps most irritating, is the strong dependence on the filling factor. It is possible that on a scale much less than an arcsecond or a kiloparsec the radiation is clumpy or filamentary. This would result in much greater local energy densities and less total energy.

Taking $k = 1, \eta = 1, \sin\phi = 1, \nu_1 = 0.01$ GHz, $\nu_2 = 100$ GHz, $\alpha = -0.8$ we obtain approximate expressions for the minimum energy condition,

$$B_{\rm me} \simeq 1.4 \times 10^{-4}(1+z)^{1.1}\nu_0^{0.22}\left[\frac{F_0}{\theta_x\theta_y s}\right]^{2/7} \text{ gauss}, \tag{3}$$

$$u_{\rm me} \simeq 1.9 \times 10^{-9}(1+z)^{2.2}\nu_0^{0.44}\left[\frac{F_0}{\theta_x\theta_y s}\right]^{4/7} \text{ erg cm}^{-3}. \tag{4}$$

The minimum energy condition is particularly sensitive to angular size. Because of the limited range of brightnesses that can be studied with a particular instrument, values of $B_{\rm me}$ derived from measurements made with the same telescope usually do not differ by much more than a factor of four or five. Typical values obtained for $B_{\rm me}$ are $\sim 10^{-6.5}$ for cluster halos, $10^{-5.5}$ G for the diffuse lobes, $\sim 10^{-5}$ G for the hot spots, and $\sim 10^{-3}$ G for the tiny flat spectrum cores. Resultant total source energies can reach 10^{60} ergs. However, it must be stressed that there is little evidence that the minimum energy condition is actually obeyed.

3.1.2 SOURCE CONFINEMENT In order to account for the nonspherical shapes of radio sources the particles and field must be prevented from dispersing at the relativistic internal sound speed of $c/\sqrt{3}$. The pressure exerted by the relativistic gas in the radio source, $u/3$, must therefore be balanced by some pressure, P, or by inertial drag. Several mechanisms have been considered for confinement (see, for example, Longair et al. 1973, Pacholczyk 1977) and in each case the pressure balance condition can be used to calculate limits for the various parameters that characterize the resisting forces.

Table 1 Some possible confinement mechanisms

	Mechanism	Approximate Restriction
Internal:	Gravitational: Point mass M at center of spherical source, diam. θ (arcsec), distance D (Mpc)	$M \geq 7 \times 10^{7}(D\theta)^{2}B_{me}M_{\odot}$
	Inertial: Blob, translational velocity, v_t Source separation/component size, R/r	$\rho_{int} \gtrsim 3 \times 10^{-22}(R/r)^{2}B_{me}^{2}(v_t/c)^{-2}$ gm cm^{-3}
External:	Static thermal: Temperature T	$\rho_{ext}T \gtrsim 2.5 \times 10^{-10}B_{me}^{2}$ gm cm^{-3} deg
	Dynamic: Ram pressure, translational velocity v_t	$\rho_{ext} \gtrsim 7 \times 10^{-23}B_{me}^{2}(v_t/c)^{-2}$ gm cm^{-3}
	Magnetic	$B_{ext} \gtrsim B_{me}$

Some possible confining mechanisms are listed in Table 1 together with the restrictions implied by pressure balance. Their applicability to the various regions of radio sources will be considered in Section 4. In real life several of these processes may be occurring simultaneously, and the detailed hydrodynamic interactions will probably result in a considerably more complicated situation than can be treated by simple static-pressure balance arguments.

3.1.3 MAGNETIC FIELD FROM COMPARISON WITH X RAYS An independent method of obtaining information about the distribution of magnetic field strengths in extended sources is based on the fact that the same relativistic electrons that produce the radio synchrotron emission will scatter photons of the microwave background to X rays. The ratio between radio and X-ray surface brightness depends on the magnetic field strength (Perola & Reinhardt 1972, Bridle & Feldman 1972, Costain et al. 1972, Harris & Romanishin 1974, Harris & Grindlay 1979). The process is reviewed by Gursky & Schwartz (1977).

The expression for the resultant magnetic field strength given by Harris & Grindlay (1979) can be approximated to within about $\pm 10\%$ between $-0.6 > \alpha > -1.4$ and rewritten as

$$B = \{6.6 \times 10^{-40}(4800)^{\alpha}(1+z)^{3-\alpha}F_R F_x^{-1}\nu_R^{-\alpha}E_x^{\alpha}\}^{1/1-\alpha}\,\text{gauss} \quad (5)$$

where F_R is the radio flux density (in Jy) at frequency ν_R (GHz), F_x is the X-ray flux (erg cm^{-2} Hz^{-1}) at energy E_x (keV), α is the spectral index ($F_R \propto \nu_R^{\alpha}$), and z is the redshift.

The main problems in using this method to determine the magnetic field strengths in extended radio sources arise from the required X-ray surface brightness sensitivity and the difficulty of separating possible inverse Compton X rays from the thermal X-ray distribution. However, one can at least obtain an upper limit for the inverse Compton contribution and hence a lower limit on the magnetic field strengths. Until now this has been done using only a few relatively low resolution X-ray measurements. For Centaurus A Cooke et al. (1978) obtained $B \gtrsim 7 \times 10^{-7}$ G and for Cygnus A Fabbiano et al. (1979) obtained $B \gtrsim 1.6 \times 10^{-6}$ G indicating that the extended lobes are not too far from equipartition. With high sensitivity X-ray observations and resolution comparable to the radio maps, this method promises to provide more information about magnetic fields in extended radio sources. A beginning is now being made with the Einstein Observatory, which, although providing an enormous improvement in X-ray sensitivity and resolution, can detect extended inverse Compton emission only from a few of the strongest sources.

3.1.4 AGES—IN SITU ACCELERATION A problem frequently considered in discussions of source morphology concerns the place where the observed synchrotron electrons are accelerated. Does this occur entirely in the nucleus, mainly in the hot spots, or is there an accelerating process at work throughout the entire source?

For the acceleration to have taken place at an angular distance θ (arcsec) from where the radiation is observed, the electron must have traveled to its present position in time,

$$t_d = 4.7 \times 10^6 D_\theta \theta v^{-1} (\sin \psi)^{-1} \text{ yr}, \tag{6}$$

where D_θ (Mpc) is the "angular size" distance (McVittie 1965), v (km s^{-1}) is the velocity at which electrons travel from the nucleus to the position under study, ψ is the angle between this direction and the line of sight. For an isotropic distribution of pitch angles the average age of a radiating synchrotron electron, t_r, is (van der Laan & Perola 1969, De Young 1976)

$$t_r = 0.82 B^{1/2} (B^2 + B_R^2)^{-1} (1+z)^{-1/2} \nu_*^{-1/2} \text{ yr} \tag{7}$$

where B (G) is the magnetic field strength in the source, $B_R = 4 \times 10^{-6} (1+z)^2$ G is the equivalent magnetic field strength of the microwave background. ν_* (GHz) is the frequency above which an exponential drop in flux will occur, and usually exceeds ν_0, the observing frequency. A necessary condition for acceleration to have occurred at a distance θ is $t_d = t_r$, i.e.

$$5.7 \times 10^6 D_\theta \theta v^{-1} (\sin \psi)^{-1} B^{-1/2} (B^2 + B_R^2)(1+z)^{1/2} \nu_*^{1/2} < 1. \tag{8}$$

To apply this condition we need to have some information about v and B. Of course we can always take $v < c$, but in most cases there is evidence that the velocities are considerably smaller. If we accept the radio-trail hypothesis (Section 2.2.1), for tailed sources v is the velocity of the parent galaxy. A reasonable upper limit to v of a few thousand km s^{-1} is then given by the distribution of radial velocities of galaxies in the cluster. Likewise, for the lobes of double sources, the observed asymmetry has been used as a statistical argument that the outward electron velocities are smaller than 0.2 c (Sections 4.2 and 4.4). An additional possible upper limit to the velocities is the generalized sound speed in the source $(u/\rho)^{1/2}$ which in the equipartition case reduces to the Alfvén velocity $B/(4\pi\rho)^{1/2}$. However, this is less certain since resonant damping by thermal protons in the source might permit considerably higher velocities (Holman et al. 1979).

There are two ways of specifying B. The first is to assume that the minimum energy ($\sim$ equipartition) condition holds and to calculate B from (2) or (3). The weaknesses of this approach are the lack of evidence for equipartition and the uncertainties in the formulas. (Note that minimum energy does not imply minimum B.) Also, the assumption that the pitch

angles θ are isotropically distributed may be invalid. In that case one must replace B by $B_\perp = B \sin \phi$, so electrons flowing along the magnetic field lines will suffer smaller energy losses and have prolonged lives (Spangler 1979).

One can avoid most of these limitations by choosing $B = B_R/\sqrt{3}$, the value that gives a maximum radiative lifetime (van der Laan & Perola 1969). The necessary condition for remote acceleration then becomes

$$8.0 \times 10^3 (1+z)^{3.5} v_*^{1/2} D_\theta \theta v^{-1} < 1. \quad (9)$$

In Section 4 evidence will be presented that localized particle acceleration in radio sources may be widespread and almost certainly occurs in jets where optical emission has been seen. An imaginative assortment of complicated mechanisms has been invoked to produce this in situ acceleration (see, for example, Pacholczyk & Scott 1976, Lacombe 1977, Blandford & Ostriker 1978, Eichler 1979, Eilek 1979, Ferrari et al. 1979, Smith & Norman 1979), but in view of the many assumptions and free parameters inherent in these models, they will not be discussed here.

3.2 *Polarization Distributions*

In the absence of a thermal plasma, synchrotron radiation is polarized orthogonally to the magnetic field direction by a percentage $100[(3-3\alpha)/(5-3\alpha)]\,[(B_u^2/(B_u^2+B_r^2)]$ where α is the spectral index ($S \propto \nu^\alpha$), and B_u and B_r are the respective field strengths of the uniform and random components of the magnetic field (Gardner & Whiteoak 1966, Moffet 1975). Hence simple inspection of the polarization distributions should apparently give information about the direction and turbulence of the magnetic field in a source. However, at all but the shortest wavelengths the interpretation of polarization distributions is made both more complicated and more informative by Faraday rotation. In a magnetoionic medium the plane of polarization of linearly polarized radiation is rotated through an angle $\Delta\chi$ proportional to the square of the wavelength: $\Delta\chi = 5.73 \times 10^{-3}\, R\lambda^2$ deg, where $R = 812 \int n_t(s) B_{\|}(s)\, ds \sim 8.1 \times 10^8 n_t B_{\|} s$ rad m^{-2} is the "rotation measure", λ(cm) is the wavelength, s (kpc) is the path length through the medium, $n_t(s)$ (cm^{-3}) is the density of thermal electrons, and $B_{\|}(s)$ is the component of magnetic field parallel to the path, i.e. in the line of sight.

Integrated rotation measures have been published for several hundred sources (Vallée & Kronberg 1975, Haves 1975). Although a small proportion of sources such as 3C 123 and 3C 427.1 have intrinsic rotation measures that probably exceed several hundred rad m^{-2} (Kronberg & Strom 1977, Riley & Pooley 1978), more than three quarters have absolute values smaller than 50 rad m^{-2}. Hence, the directions indicated by the

measured polarization distributions for $\lambda \lesssim 6$ cm will usually be within 10° of the unrotated angles (i.e. perpendicular to the uniform magnetic field projected on the plane of the sky). Maps of projected magnetic field directions $B_\perp$ are therefore relatively easy to produce from polarization distributions measured at short wavelengths.

In principle, a comparison of polarization distributions at several wavelengths gives the distribution of R across a source and hence information about variations in $n_t B_\parallel$. Unfortunately, matters are complicated by (*a*) ambiguities in R due to the limited number of observing frequencies, (*b*) difficulties in separating the in-source contribution to R from foreground rotation, (*c*) uncertainties in the path length s through the source, (*d*) effects of nonuniformity of the magnetic field within the source, including field reversals, (*e*) smearing due to the presence of several independent "cells" within the same observing beam.

Until now most multifrequency polarization mapping has been carried out using two (or, in a few special cases, three) observing wavelengths λ_1, λ_2. There is consequently an ambiguity of $n\pi$ in χ and a corresponding ambiguity in R of $3.14 \times 10^4/(\lambda_2^2 - \lambda_1^2)$ rad m^{-2}.

Separation of the rotation that occurs within the source from that in the foreground has been attempted in two ways. First, the foreground rotation is obtained as the average of integrated rotation measures of several nearby sources. Second, one ignores the component of rotation that is constant across the source and examines only point-to-point variations in R, on the assumption that all these relatively small-scale changes in R are produced within the source.

One can guess at the path length s using symmetry arguments and assumptions about the distance, as in the preceding discussion of the derivation of the minimum-energy conditions.

A proper treatment of the effects of a tangled magnetic field and of beam smearing must take into account the distribution of the percentage polarization as a function of wavelength. The complex polarization as a function of wavelength can be evaluated in terms of source parameters (Burn 1966, Gardner & Whiteoak 1966). To obtain meaningful information from available data, an unduly large number of assumptions must be made about the statistical properties of the inhomogeneities and the source geometry. Such analyses have been carried out for 3C 465 (van Breugel 1980c) and Virgo A (Forster 1980). A slightly different (Monte Carlo) model fitting procedure has been used by Burch (1979b) in a study of 3C 47, 3C 79, 3C 219, 3C 234, 3C 300, 3C 382, and 3C 430. The results (electron densities of from 10^{-5} to 10^{-3} cm^{-3} corresponding to total masses of $\sim 10^{11}\ M_\odot$) are all quite similar to those given by back of the envelope calculation using the simple formulas in this section. However, the more sophisticated

analyses illustrate that multifrequency polarization comparisons made, using many more frequencies than now available, could furnish useful information about the intrinsic distribution of n_t and B *along the line of sight*.

4 THE BUILDING BLOCKS OF EXTENDED RADIO SOURCES

> The fundamental cause of the development of a thing is not external but internal; it lies in the degree of contradiction within the thing.
>
> Mao tse Tung, "On Contradiction"

4.1 *Diffuse Emission*

Most radio sources are associated with some diffuse emission. The low-brightness extremities of tailed sources and narrow relaxed doubles have similar diffuse appearances, and the wide doubles have relaxed amorphous lobes. In edge-brightened doubles the diffuse emission takes the form of low-brightness bridges reaching from the outer hot spots towards the nuclei, but the distinction between bridges and radio jets (Section 4.4) is not always clear.

4.1.1 PROPERTIES The diffuse emission is characterized by a relatively steep spectrum ($-0.7 \gtrsim \alpha \gtrsim -1.2$). For tails the spectrum is sometimes observed to steepen with distance from the parent galaxy, indicating that radiative losses of the type treated in Section 3.1.4 may be occurring (e.g. Miley 1974, Schilizzi & Ekers 1975, Valentijn & Perola 1978). Similar behavior has been observed in the edge-darkened double 3C 31. However, the form of the spectral steepening in this source, one of the few that has been mapped at more than two frequencies, is not that expected from simple synchrotron losses (Burch 1977b). In contrast to the spectral variations observed in the low luminosity sources, spectral steepening has been reported in an inward direction, away from the outer edges of some edge-brightened doubles (Burch 1977a,b, 1979a,b, Dreher 1979, Högbom 1979) but not others (Jenkins & Scheuer 1976, Gopal-Krishna 1977, Gopal-Krishna & Swarup 1977).

Despite the spectral steepening that is sometimes observed, application of the arguments in Section 3.1.4, with the equipartition proviso, suggests that localized particle acceleration occurs frequently in tails (e.g. Wilson & Vallée 1977, Hintzen et al. 1977, Ekers et al. 1978b, Baggio et al. 1978, Simon 1979, Downes 1980) and also throughout the lobes of some double sources (Burch 1977b, Willis & Strom 1978, Strom & Willis 1979, Burch 1979b, van Breugel 1980a).

Fine structure is often seen in the bridges of edge-brightened doubles. These enhancements may correspond to periods of increased activity in the nuclear history, or pinpoint regions where localized particle acceleration is occurring. High sensitivity measurements of the wide double 3C 310 have also revealed weak fine structure on a scale of a few kiloparsecs within its diffuse lobes (van Breugel 1980a).

The diffuse emission is usually highly polarized with polarizations often approaching 60% at frequencies above 1 GHz indicating the presence of a well-ordered magnetic field (Section 3.2). The field direction is generally observed to be circumferential (e.g. Fomalont 1972, Miley & van der Laan 1973, Strom et al. 1978, Willis & Strom 1978, Andernach et al. 1979, Burch 1979b, De Young et al. 1979, van Breugel 1980a, Strom & Willis 1979). See also Figures 1, 3, and 5. For the diffuse bridges and tails the known polarization directions therefore indicate *average* fields directed along the components (e.g. Miley 1976, Miley et al. 1975, Högbom 1979, Burch 1979b), although locally the magnetic field directions are often more complex, particularly near regions of enhancement in total intensity.

4.1.2 CONFINEMENT AND SHAPING How are the diffuse emitters held together? Evidence that the confining agent is thermal pressure of a hot gas comes from X-ray measurements (e.g. Gursky & Schwartz 1977, Mushotzky et al. 1978), which show that, at least in some of the rich clusters that house radio sources with diffuse lobes, there is an intergalactic medium with $\rho \sim 10^{-27.5}$ g cm^{-3} and $T \sim 10^{7.5}$ K. By the arguments of Section 3.1.2 the pressure of such a gas would be sufficient to confine the lobes provided their internal energy is not much greater than the minimum permitted values ($B_{me} \sim 10^{-5.5}$ G). If thermal pressure does indeed confine tails, the discovery of two tailed galaxies in poor clusters (Ekers et al. 1978b) suggests either that an intergalactic density of $\sim 10^{-27.5}$ gm cm^{-3} may be widespread in the Universe or, as is perhaps more likely, that the sources are confined by giant circumgalactic gaseous halos with dimensions comparable with or larger than the extended radio emission (Norman & Silk 1979).

One of the properties of the diffuse emission that has received considerable attention is the curvature frequently occurring in the tails of tailed radio galaxies. Significantly curved tails have been observed in 3C 83.1B, 3C 129 (Miley et al. 1972, Miley 1973), IC 711 (Vallée & Wilson 1976, Wilson & Vallée 1977), 5C 4.81 (Jaffe et al. 1976), 1200+519/4C 51.29, and 1700+397/4C 39.49 (Miley & Harris 1977). Several explanations have been proposed for this curvature—all within the context of the radio-trail model (Section 2.2.1). It has been suggested that the tail traces a curved orbit of the parent galaxy in the gravitational field of the cluster (Miley et al. 1972) or of

a neighbouring galaxy (Byrd & Valtonen 1978). Alternatively, the tail may be distorted by large-scale shear in the velocity field of the intergalactic gas (Jaffe & Perola 1973) or by buoyancy forces in the gravitational field of the cluster (Cowie & McKee 1975). Probably more than one of these mechanisms contributes to bending radio tails. Interpretation of the observations is complicated by effects of projection.

Buoyancy is a particularly interesting possibility. It would cause tails lighter than their surroundings to rise away from the cluster centers. According to Cowie & McKee (1975) denser "detached plasmoids" may be left behind in this process. This may be occurring in the case of 3C 83.1B/NGC 1265 in the Perseus Cluster whose low brightness structure is shown in Figure 8. It has been suggested (Gisler & Miley 1979) that the weak extension to the northeast is such a "heavy tail," which traces the actual orbit of NGC 1265, while the main body of the tail has been bent

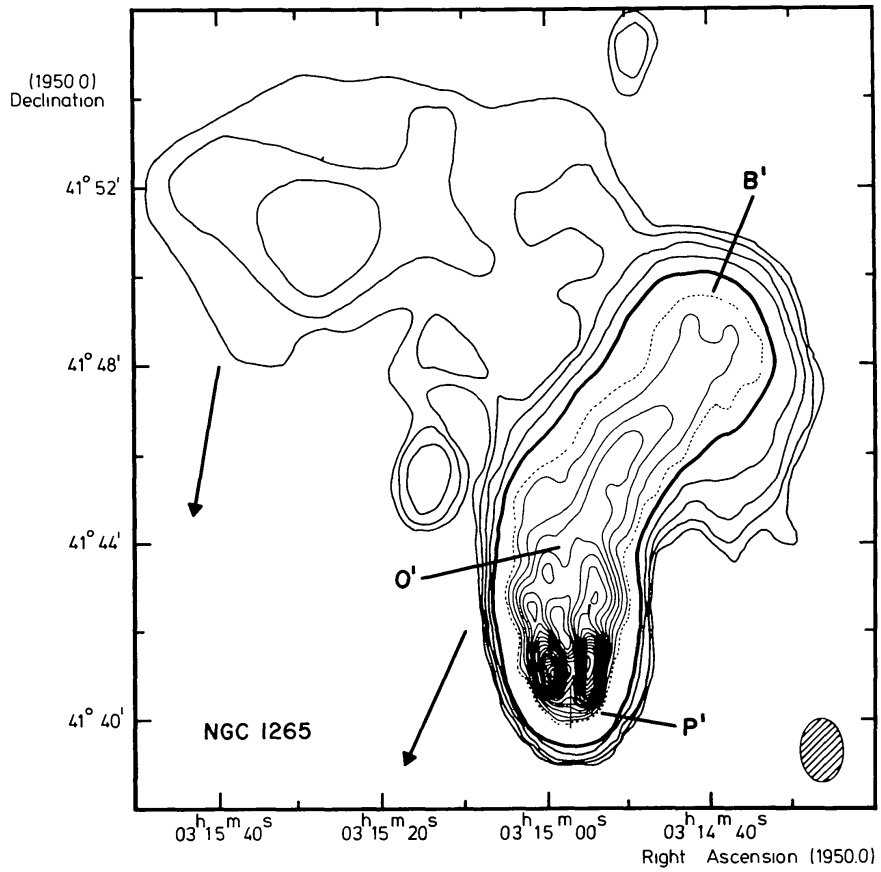

Figure 8 3C 83.1B/NGC 1265, the outer contours are from Westerbork 0.6-GHz intensity measurements and the inner contours were taken from higher resolution 1.4-GHz data (from Gisler & Miley 1979). The cross shows the position of the nucleus of NGC 1265 and the arrows indicate the direction to the center of the Perseus Cluster. The weak northeastern extension may represent the trajectory of the galaxy and the main tailed structure a buoyant tail floating away from the center of the Perseus Cluster.

away from the cluster center by buoyancy forces. On this basis, making several additional assumptions about the geometry, one obtains a lower limit to the mass of the Perseus Cluster of $\sim 10^{15}\ M_{\odot}$, similar to that obtained independently from the virial theorem. There are also indications that buoyancy plays a part in shaping the structures of diffuse emission in double radio galaxies, e.g. 3C 264, 3C 315 (Northover 1976), and 3C 449 (Bystedt & Högbom 1979).

4.2 *Hot Spots*

As we have seen in Section 2.2.1, hot spots occur at the outer edges of the most luminous sources and are sometimes seen within the diffuse lobes of the weaker ones.

4.2.1 PROPERTIES Hot spots have sizes that are typically a few kpc (see, for example, Readhead & Hewish 1976, Kapahi 1978). Hot spots in opposite lobes are usually collinear with the central radio core (Section 2.1.1). There are suggestions from the scintillation data that hot spots occur less frequently in sources whose overall sizes are larger than ~ 200 kpc (Readhead & Hewish 1976), or alternatively that the hot spots in the larger sources are bigger.

Hot spots have spectra similar to or slightly flatter than the surrounding diffuse emission (e.g. Hargrave & Ryle 1976, Jenkins & Scheuer 1976, Gopal-Krishna 1977, Gopal-Krishna & Swarup 1977, Burch 1977a, Spangler & Meyers 1978, Högbom 1979, Burch 1979b). Their integrated polarizations at frequencies above 1 GHz are typically 20–30% (see Hargrave & Ryle 1974, Strom & Willis 1979). Circumferential magnetic fields are indicated (see, for example, Dreher 1979) with the average direction of the magnetic field usually oriented roughly perpendicular to the overall extent of the radio component.

Although the presence of hot spots is clearly connected with the total radio-source luminosity, studies of the variation of hot-spot properties with luminosity are difficult to carry out. Such studies are largely confined to the most luminous and distant sources for which cosmological effects are important. The best-established correlation is undoubtedly the increase with luminosity of the separation of the hot spots from their parent nuclei (Section 2.2.3). Less credence should be given to the report that the average hot spot size increases with luminosity (Readhead & Hewish 1976). The initial interpretation of the (scintillation) data on which this report was based has been contradicted by high resolution interferometry (Kapahi & Schilizzi 1979).

During the last few years there have been several searches for optical emission from hot spots. Evidence has been found for such emission in 3C

285 (Tyson et al. 1977), in 3C 265 and 3C 390.3 (Saslaw et al. 1978), in 3C 33 (Simkin 1978), and in NGC 7385 (Simkin & Ekers 1979). The observed radio polarizations of the hot spots would argue against a thermal origin for the optical emission (Saslaw et al. 1978), although in the case of 3C 33 Simkin has claimed that there may be weak emission lines present. The most plausible mechanisms for producing the optical emission would be direct synchrotron radiation or inverse Compton scattering of the microwave background by the electrons that produce the radio emission (Saslaw et al. 1978).

4.2.2 ORIGIN The collinearity of the hot spots with the nucleus in some double radio sources (Section 2.1.1) indicates that hot spots play a fundamental role in the radio-source phenomenon. It has been suggested that they are (*a*) regions where acceleration of electrons to relativistic energies occurs through energy pumped in from the nucleus (e.g. Rees 1971), (*b*) places where the bulk kinetic energy of the relativistic electrons created in the nucleus is thermalized to produce visible radiation (e.g. Blandford & Rees 1974), (*c*) the accumulation of plasmons, multiply ejected from the nucleus and decelerated by ram pressure (Christiansen et al. 1977), or (*d*) the location of compact supermassive objects ejected from the nucleus which produce and accelerate the relativistic electrons through interaction with circumgalactic gas (Saslaw et al. 1974).

In the first two cases the hot spots represent the end of a beam and they move outwards from the nucleus as the beam rams through the ambient medium. Although the hot spots need not be strictly "confined" in such a situation their motion will be governed primarily by ram pressure forces (e.g. Blandford & Rees 1974), and from the arguments of Section 3.1.2 an external medium with a density of $\rho_{ext} \gtrsim 10^{-28}$ gm cm^{-3} is needed. This lower limit was calculated using an upper limit of 0.1 c for the outward velocities of the hot spots, since for much greater outward speeds relativistic effects would result in a higher proportion of very unequal doubles than is observed (Mackay 1971, Katgert-Merkelijn et al. 1980, Longair & Riley 1979). Similar confinement arguments apply to the multiple-plasmon models.

To hold the hot spots together by gravitation (Burbidge 1967, Callahan 1976, Flasar & Morrison 1976) requires compact objects of mass $\gtrsim 10^9$ $M_\odot$. This is unlikely. First, there is no evidence for structure in the hot spots on a scale much smaller than a kiloparsec. Second, in order to explain the observed alignment of the extended emission with the cores (Section 4.3.3), and with the optical galaxies and quasar polarizations (Sections 5.3), a polar ejection mechanism for the multiple ejection of compact objects from the nucleus is required. The slingshot process (Saslaw et al. 1974), the only

mechanism to have been proposed for such ejection, is equatorial and therefore does not preserve memory of direction. Moreover it has difficulty in explaining the detailed brightness distributions of head-tail galaxies (see, for example, Downes 1980). Attempts to reconcile this theory with observations (e.g. Valtonen 1977) appear contrived.

4.3 *Cores*

4.3.1 TWO TYPES OF CORES Core emission in extended radio sources is of two types. First, there are the ultracompact flat-spectrum ($\alpha < -0.4$) components with sizes $\ll 1$ pc buried deep in the nuclei of the parent galaxies or QSOs. These components have similar properties to the (isolated) compact variable sources (Kellermann 1978). During the last decade compact cores have been shown to be present in extended radio sources of every morphological type. Flat-spectrum radio cores also frequently occur in the nuclei of elliptical and SO galaxies that are not extended radio sources (Ekers 1978, Crane 1979), and at a weaker level in some spirals (de Bruyn 1978). Even our own galaxy has a tiny flat-spectrum component near its center (Oort 1977 and references therein).

Second, about a quarter of the cores found in radio galaxies have steep spectra with indices smaller than -0.4 (Bridle & Fomalont 1978). These have typical sizes of a few kpc and are clearly different from the ultra-compact cores. The best-studied examples are in galaxies—Virgo A/M 87 (Turland 1975a, Forster et al. 1978), Fornax A (Geldzahler & Fomalont 1978), and the giant edge-brightened double 3C 236 (Fomalont & Miley 1975, Fomalont et al. 1979, Schilizzi et al. 1979). A steep-spectrum core has also been found in the quasar 3C 207 (Joshi & Gopal-Krishna 1977). The steep-spectrum cores in Virgo A and 3C 236 have been mapped in detail and in both cases they have basically double structure with compact flat-spectrum cores imbedded within them. The limited information available suggests that the spectral index distribution across steep-spectrum cores is remarkably constant (Berlin et al. 1975, Fomalont et al. 1979). Steep-spectrum cores having the steepest spectra tend to be the most luminous (Bridle & Fomalont 1978); a similar behavior is observed for the integrated luminosities and spectra of extended sources (e.g. Blumenthal & Miley 1979). Isolated steep-spectrum sources with sizes of a few kiloparsecs but no detectable extended emission frequently occur in spiral and Seyfert galaxies (Ekers 1978, de Bruyn & Wilson 1978). Despite the similarities it is not clear whether these isolated sources have any connection with the steep-spectrum kiloparsec cores in extended radio sources.

Since radio-core emission is almost certainly an indication of relatively recent nuclear activity, we may glean information about radio-source evolution by investigating possible relationships between the cores and the associated extended emission.

4.3.2 CORE LUMINOSITIES First we shall examine the relative strengths of cores in different types of extended radio sources. For many sources, measurements are of insufficient resolution to separate the flat- and steep-spectrum cores. Therefore, most studies have been made using combined core fluxes. Neither Fanti & Perola (1977) nor Bridle & Fomalont (1978) find evidence that the core luminosity, P_{core}, increases with that of the extended emission, P_{ext}, for radio galaxies, although Fanti & Perola cannot exclude a weak dependence.

Extended radio sources associated with QSOs tend to have relatively more powerful radio cores than those associated with galaxies (Ekers & Miley 1977, Riley & Jenkins 1977, Miley & Hartsuijker 1978, Owen et al. 1978b). Further data (G. K. Miley, T. Heckman, and R. Fanti, in preparation) indicates that extended quasars have cores that are on average about a factor of twenty stronger than radio galaxies having the same total luminosity. In addition, there appears to be a weak dependence of the core luminosity on the extended emission ($P_{\text{core}} \propto P_{\text{ext}}^{1/2}$) which would be consistent with the earlier work of Fanti & Perola (1977).

4.3.3 CORE STRUCTURES In several cases the core structures have been determined, primarily with VLBI techniques, and the morphologies of the cores have been related to those of the extended emission. This has been done for the flat-spectrum cores in Cygnus A (Kellermann et al. 1975), 3C 111 (Pauliny-Toth et al. 1976), 3C 273 and 3C 345 (Readhead et al. 1979), 3C 390.3 (E. Preuss et al., in preparation), NGC 6251 (Readhead et al. 1978b, Cohen & Readhead 1979), Virgo A/M 87 (Kellermann et al. 1977 and references therein), and 3C 84/NGC 1275 (Pauliny-Toth et al. 1976), and for the steep-spectrum cores in 3C 236 (Wilkinson 1972, Fomalont & Miley 1975, Fomalont et al. 1979, Schilizzii et al. 1979), Virgo A/M 87 (Turland 1975a, Forster et al. 1978), Centaurus A/NGC 5128 (Christiansen et al. 1977), and 3C 84/NGC 1275 (Miley & Perola 1975).

For the narrow sources whose extended emission is linear and symmetrically distributed (e.g. Cyg A, 3C 111, 3C 236, 3C 390.3, NGC 6251) the cores are observed to be *aligned* to within a few degrees of the outer lobes, even though the scales involved differ by as much as 5×10^6. Assuming the core emission to have been produced by relatively recent nuclear activity allows one to conclude that the orientation of the nuclear powerhouses must have remained fixed throughout the lifetimes of these sources. For the giant sources 3C 236 and NGC 6251 the light travel time from their nuclei to their outer edges is $\sim 10^7$ yr implying a memory for direction in excess of this time. The only relevant direction that could feasibly remain fixed for such a long time is the angular momentum axis of a rotating compact object buried in the nucleus. Despite the overall agreement between the position angles of the core and extended structures in those sources there are fine-

scale misalignments of a few degrees apparent both in the steep-spectrum core of 3C 236 (Fomalont & Miley 1975, Schilizzi et al. 1979) and in the flat-spectrum core of NGC 6251 (Cohen & Readhead 1979). These may reflect bending in the cores similar to the wiggles observed in some radio jets (Section 4.4.2).

In contrast to the aligned cores in symmetric narrow sources, the four known cases of sources with one-sided extended emission (S or D2 sources in Section 2.1.1) have compact cores that are considerably bent (Readhead et al. 1978a). Two explanations have been proposed for this misalignment of cores in asymmetric sources. First, the cores may be bent by a pressure gradient in the nucleus. Second, a slight bending in the core might be apparently magnified if the radiating particles were moving at relativistic

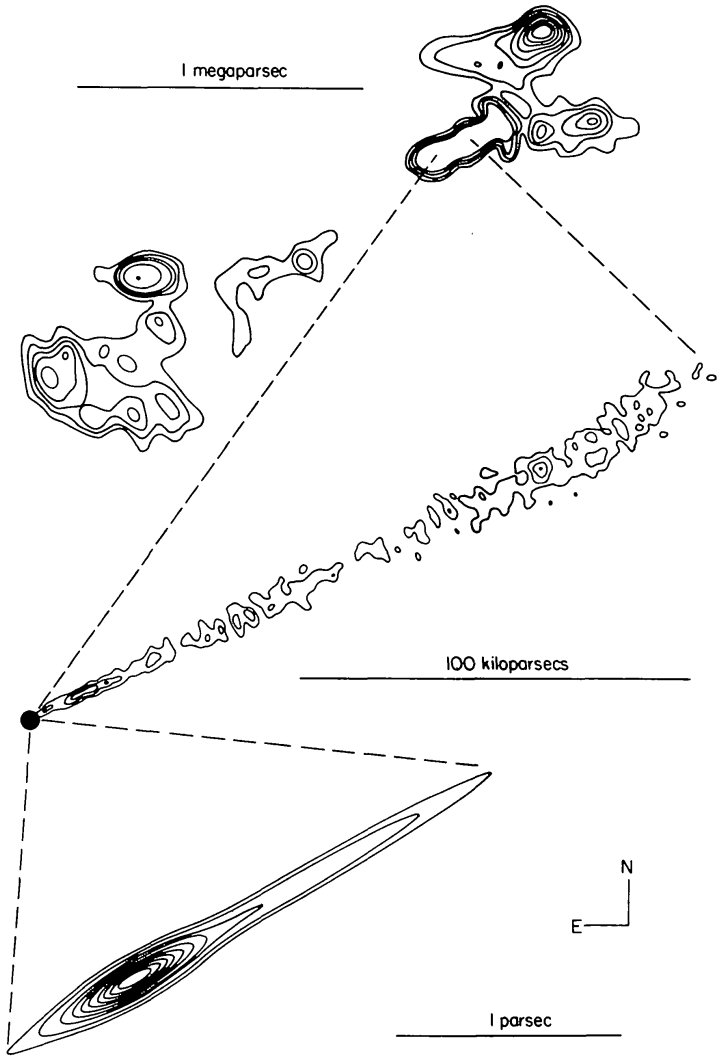

Figure 9 The radio source associated with NGC 6251 showing the alignment of the core and jet relative to the overall source structure (from Readhead et al. 1978a and kindly supplied by Marshall Cohen).

speeds along a narrow beam pointing approximately in our direction (Scheuer & Readhead 1979).

So far we have only considered the structure of cores in narrow sources. For the two wide doubles for which there is information, the cores and the extended structures are grossly misaligned, in Virgo A/M 87 by $\sim 70°$ and in Centaurus A/NGC 5128 by $\sim 45°$. It is possible that the nuclear axes of the wide sources change appreciably during the source lifetime (Miley 1976). Alternatively there may be a shearing pressure gradient in the medium surrounding these galaxies which disrupts the beam and distorts the morphology of the outer extended radio emission. Such a process may well be occurring in 3C 84/NGC 1275 which has a radio core that is aligned on scales of a parsec to 2 kpc but whose extended emission is completely amorphous. 3C 84 is located at the center of the Perseus Cluster, which X-ray observations indicate contains some of the densest and hottest gas of any known cluster. Virgo A and Centaurus A also have strong X-ray halos.

4.4 *Jets*

Long before celestial radio sources were dreamed of, an optical jet was seen in the nebula M 87 (Curtis 1918). More than fifty years later a radio counterpart of this jet was found in the associated radio source Virgo A (Hogg et al. 1969, Wilkinson 1974, F. N. Owen and P. Hardee, in preparation). See Figure 10. The radio and optical spectra of this jet and its high optical polarization (Baade 1956, Hiltner 1959, Schmidt et al. 1978) are

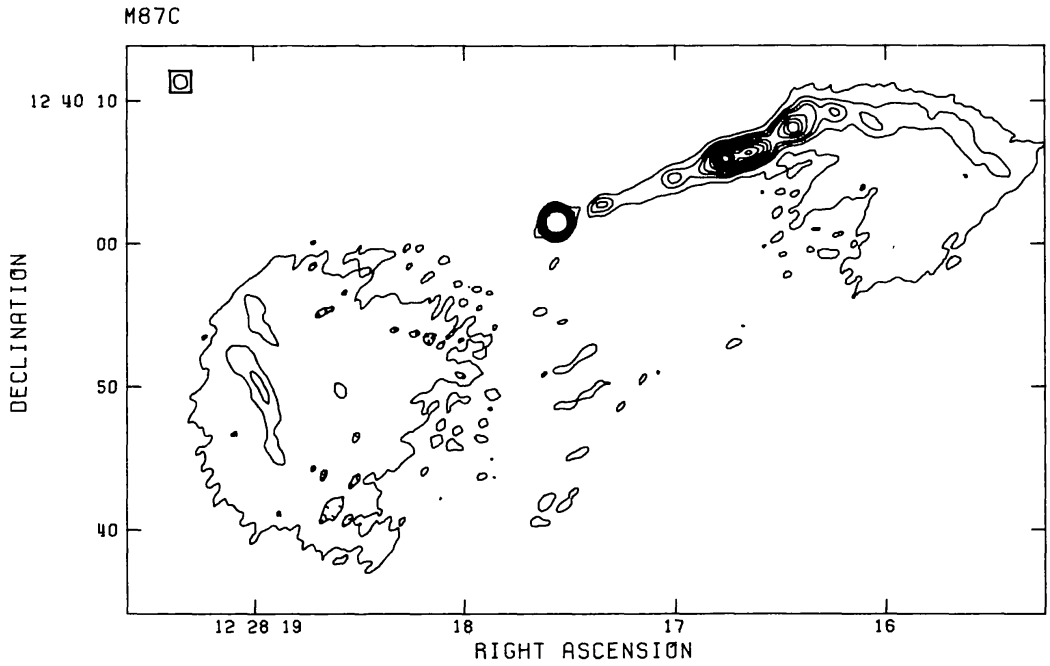

Figure 10 The jet and steep spectrum core of Virgo A/M 87 (VLA, 5 GHz) (from F. N. Owen and P. Hardee, in preparation and kindly supplied by the authors).

all indicative of nonthermal emission. On the identification of 3C 273, the brightest known quasar, an optical jet was also seen in the direction of the extended radio emission (Hazard et al. 1963). For several years no further examples of jets were recognized; M 87 and 3C 273 were regarded as exceptional, but in fact their most exceptional property is probably their proximity.

The situation changed in the mid-seventies. Long narrow radio structures were found to emanate from the nuclei of the radio galaxies 3C 219 (Turland 1975b) and B 0844+31 (van Breugel & Miley 1977) and it was realized that analogous jet-like structures were also present at the heads of several tailed galaxies (van Breugel & Miley 1977). Several additional examples of jets were then recognized and at the time of writing about twenty radio jets are known. Some of the most prominent examples are in the double sources NGC 315 (Bridle et al. 1976, Bridle et al. 1979a), 3C 31 (Burch 1977b, 1979c), NGC 6251 (Waggett et al. 1977), 3C 449 (Perley et al. 1979, Bystedt & Högbom 1979) B 0844+31 (van Breugel 1980b), and HB 13 (Masson 1979) and the tailed sources 3C 83.1B/NGC 1265 (Miley et al. 1975, Owen et al. 1978a), 3C 129 (van Breugel & Miley 1977, Owen et al. 1979, Downes 1980), and 3C 465 (van Breugel 1980c). Some of these are illustrated in Figures 11, 9, 12, 14, 13 and 3.

To date, most radio jets have been found in nearby relatively low

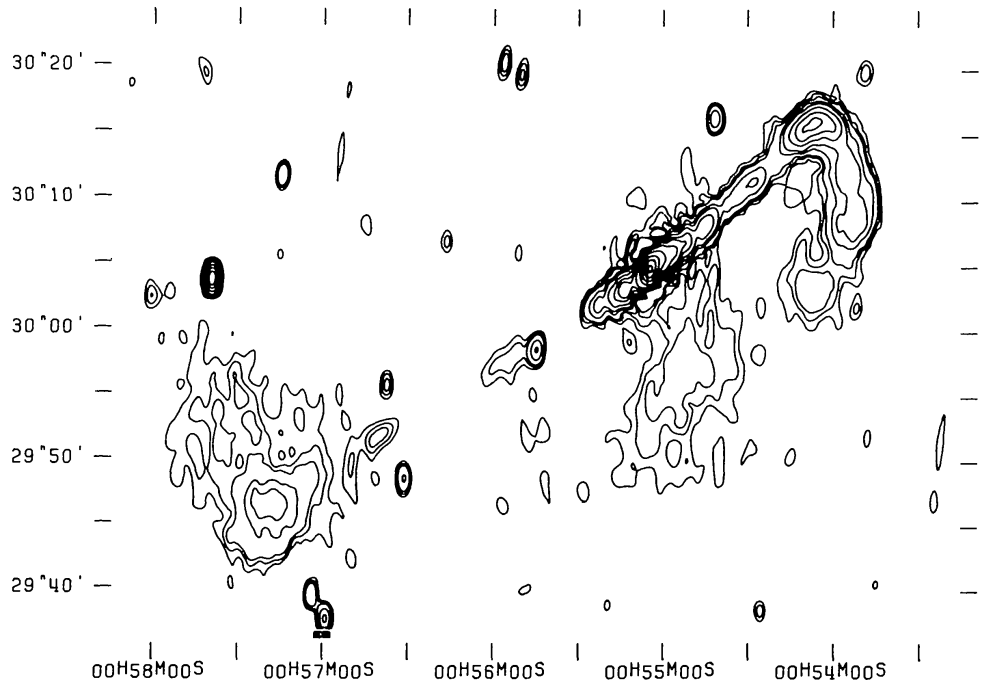

Figure 11 The 1-Mpc radio source associated with NGC 315 (Westerbork 0.6 GHz) showing the jet and its overall rotational symmetry. The cross indicates the position of the associated galaxy (from Willis 1978 and kindly supplied by the author).

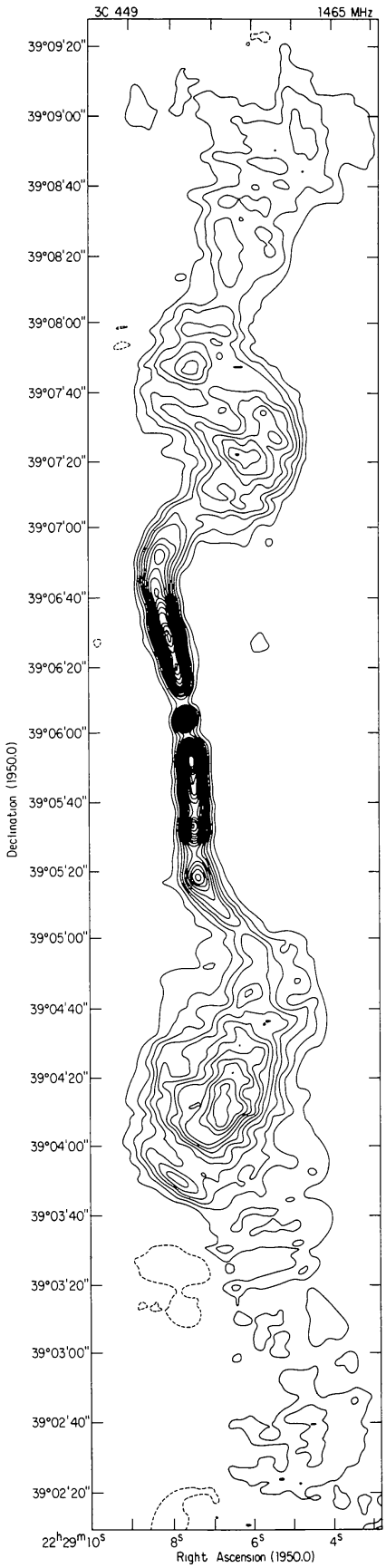

Figure 12 The inner region of 3C 449 (see Figure 2) showing the jet (VLA, 1.4 GHz) (from Perley et al. 1979 and kindly supplied by Ed. Fomalont).

luminosity sources. This may be partly because nearby sources can be studied in greater detail. However, in the more luminous edge-brightened doubles the distinction between the features previously called "bridges" and "jets" is often unclear. Several quasars, e.g. 1004+13, 1047+09, 1058+11 (Miley & Hartsuijker 1978), and 4C 32.69 (Potash & Wardle 1979) have large-scale structures reminiscent of jets. Higher resolution observations with the VLA have recently confirmed the presence of jets in 4C 32.69 (Potash & Wardle 1980) and 1004+13 (E. Fomalont and G. K. Miley, in preparation).

4.4.1 ORIGIN Before the widespread existence of jets was suspected, a considerable body of evidence had accumulated that extended radio sources are powered quasi-continuously from the nuclei of their parent galaxies (Section 1.4). Although the existence of visible jets was not explicitly predicted by models of the energy transport, it seemed logical to associate these narrow structures that emanate from the radio cores and penetrate for several hundred kiloparsecs into the radio lobes with the umbilical cords that carry the energy required to nurture the extended emission. There are several byproducts of the energy-pumping process that could produce the observed radiation. Possibilities are collisions between freshly ejected plasmons and older "relics" (Christansen et al. 1977), or shocks within a relativistic beam (Rees 1978a, Blandford & Königl 1979). Dissipation at the edges of a beam has been suggested as a possible alternative (Blandford & Rees 1978), but since there is no indication that the sides of jets are enhanced (Perley et al. 1979), this is unlikely to be the dominant process for jets in low luminosity sources.

Within the context of these various mechanisms one can list three properties of the energy transport process that may exert a dominating influence on the observed luminosities and other properties of the jets.

1. The angle that the jet is inclined to the line of sight. If the jets represent outflow at relativistic velocities one might observe a dependence of intensity on aspect (cf Rees 1978a, Blandford & Königl 1979).
2. The amount of energy being conducted to the lobes. The highly energetic processes required to generate radiation in the jets may vary sporadically as a result of unsteady nuclear activity (Rees 1978a).
3. The efficiency of the energy transport. Inefficiency may be related to the degree to which energy transport is relativistic (Rees 1978a) or to the amount of interstellar matter entrained in the beam (Blandford & Königl 1979).

There is as yet an insufficiently large sample to investigate these questions properly, but simple interpretation of some of the individual morphological

properties of jets provides several clues as to their nature and to the processes involved. Since, at the time of writing, sources containing radio jets are being studied intensively by the VLA, the following discussion is inevitably very preliminary.

4.4.2 SOME PROPERTIES The few radio jets that have been studied in detail show considerable diversity. For example, the lengths of the jets range from ~ 2 kpc in Virgo A to ~ 260 kpc in NGC 315 and their spectral indices from ~ -0.5 to ~ -0.8. Three properties of jets deserve special mention.

First, in several cases (e.g. 3C 449, 3C 83.1B/NGC 1265, NGC 315, 3C

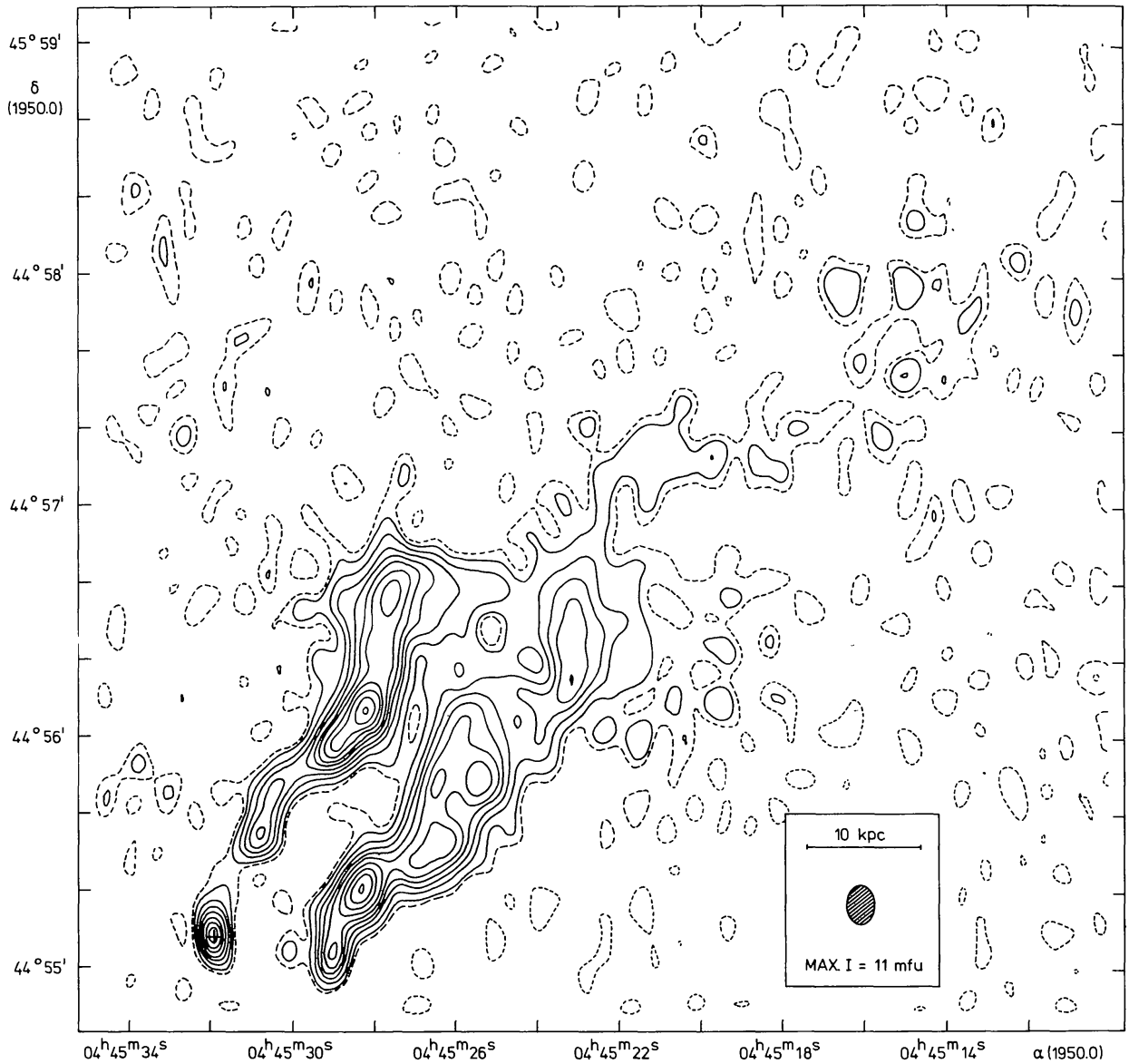

Figure 13 The head of the tailed source 3C 129 showing the symmetric wiggles (from van Breugel & Miley 1977).

219) there appear to be "gaps" of a few kpc between the nuclear core and the location where the jets are seen to begin (Perley et al. 1979). This may be caused by large variations in the power of the nuclear machine, or to more efficient and hence less visible energy transport near the nucleus due to a more highly collimated and less randomized beam of relativistic electrons.

Second, several jets are observed to have wiggles on a scale of about 30 kpc. Examples are B 0844+31 and 3C 129 (van Breugel & Miley 1977, Owen et al. 1979), 3C 31 (Burch 1977a,b, 1979a,c, Fomalont et al. 1979), 3C 449 (Perley et al. 1979, Bystedt & Högbom 1979), HB 13 (Masson 1979), and 3C 83.1B/NGC 1265 (Owen et al. 1978a). Figure 13 shows the symmetric wiggles clearly apparent in the head of the tailed source 3C 129. The wiggles have been attributed either to precessional motion of the central nuclear machine during the source lifetime (van Breugel & Miley 1977) or orbital motion of the parent galaxy (Blandford & Icke 1978, Bystedt & Högbom 1979).

Third, an intriguing aspect of jets that have been surveyed is their asymmetry. Except for 3C 449 (Perley et al. 1979) and 3C 83.1B/NGC 1265 (Owen et al. 1978a), the flux ratio between opposing jets is much larger than the flux ratio between the corresponding extended lobes (e.g. Willis et al. 1978, Cohen & Readhead 1979). Several possible explanations have been proposed to explain how asymmetric jets can power symmetric radio sources. Because of the existence of some two-sided jets the possibility that jets are accretion wakes formed by the motion of their parent galaxies through an intergalactic medium (Yabushita 1979) can be rejected. Another possibility is that the brightness of the jets (reflecting the efficiency of energy transport) may be strongly influenced by a nonuniform galactic environment, but it is not clear why the properties of the environment should differ on opposite sides of the nucleus. Third, opposing jets may have similar intrinsic intensities with the receding one apparently weakened by the Doppler effect (Rees 1978a, Blandford & Königl 1979). Typical flow velocities of $\sim 0.3\ c$ would then be implied. A powerful argument against this view is the observation that some one-sided jets bend without undergoing significant intensity changes (E. van Groningen, C. Norman, and G. K. Miley, in preparation). Fourth, the nuclear engine may flip, supplying energy to the low lobes alternately (Willis et al. 1978). Again it is not clear how this could occur. A fifth possibility is that the beam shines through a clumpy nucleus and that these clumps occasionally block the beam.

4.4.3 OPTICAL EMISSION Optical emission from jets can provide unique information about the physics involved. Since synchrotron decay times for

electrons emitting in the optical are typically ~ 10 yr, optical synchrotron features precisely locate regions where the electrons are accelerated (cf Section 3.1.4). An analogy with the optical/radio jet in M 87 prompted a deep search for optical counterparts of four other radio jets (Butcher et al. 1980). In two cases (3C 66 and 3C 31) optical jets were found with similar ratios of optical to radio emission as in M 87. These measurements suggest that a continuous nonthermal spectrum extending from $\sim 10^9$ Hz to $\sim 10^{15}$ Hz is a fairly common property of jets in radio galaxies and that acceleration of the relativistic particles occurs along the jet. The recent detection of X-ray emission from the M 87 jet (P. Gorenstein, E. Schreier, and E. Feigelson, private communication) shows that some jets emit over eight decades of frequency.

M 87 is the only nonthermal jet whose optical properties have been studied in some detail (e.g. de Vaucouleurs et al. 1968). Optical polarization measurements of the M 87 jet (Schmidt et al. 1978) show a fairly ordered magnetic field that changes direction from knot to knot. The changes in the optical polarization angle along the jet are mimicked closely by the 6-cm radio polarization angle. This suggests that the electrons that produce the optical and radio emission originate in roughly the same regions of the magnetic field and that there is little Faraday rotation within the knots. However, the optical and 6-cm radio polarization angles are offset from each other by $\sim 75°$ indicating considerable foreground rotation. The foreground rotation may be produced within the 2-kpc steep-spectrum core of Virgo A (Turland 1975a, Forster 1980) or perhaps within one of the 40-kpc extended radio lobes ($B_{\rm me} \sim 4 \times 10^{-6}$ G; Andernach et al. 1979) which coexists with the X-ray halo ($n_{\rm t} \sim 10^{-2}$ cm^{-3}; Catura et al. 1972).

Optical jets with significant thermal emission have been reported in the giant radio galaxies Centaurus A (Blanco et al. 1975, Dufour & van den Bergh 1978) and DA 240 (Burbidge et al. 1975, 1978). Although an X-ray jet has been seen in Centaurus A (Schreier et al. 1980), a radio jet has been seen in neither of these galaxies. The absence of an *observed* radio jet in Centaurus A may merely reflect the fact that this southern source is inaccessible to the most sensitive radio telescopes with sufficient resolution. Other extended radio sources in which jets may have been seen are the quasar PKS 0837-12, which has a visible extension along its radio axis (Wehinger & Wyckoff 1978), and some of the 18 candidates noted by Ghigo (1978).

4.4.4 CONE ANGLES AND MAGNETIC FIELDS/FREEDOM FOR JETS? Are the jets in pressure equilibrium with their surroundings? Model builders prefer jets to be free rather than confined. In a free jet the thermal electron density

exceeds that of the surroundings, and Kelvin-Helmholtz instabilities, which may destroy a confined jet (Blandford & Pringle 1976, Turland & Scheuer 1976), would probably be unimportant.

For a free jet the cone angle subtended at the nucleus should be constant along its length. In the giant source NGC 6251 (Readhead et al. 1978a) this angle is indeed observed to be constant over a range of more than 10^5 in length.

Also, simple arguments (Blandford & Rees 1978) predict that as a freely expanding jet widens (radius r increases) the parallel component of magnetic field should drop as r^{-2}, whereas the perpendicular component should vary only as r^{-1}. This is consistent with the magnetic field configuration observed in both 3C 31 and NGC 315 (Fomalont et al. 1980) where parallel fields close to the nucleus change to predominantly perpendicular fields after about 2 kpc. Moreover, in 3C 449 (Perley et al. 1979) and NGC 6251 (Readhead et al. 1978b) the magnetic field calculated from the minimum energy condition (Section 3.3.1) $B_{\rm me}$ scales roughly as r^{-1}, a further pointer that these jets are free, as well as weak evidence that the conditions within the jet are close to equipartition. On the assumption that the jet in 3C 449 is free and in equipartition together with several of the arguments of Section 3.1.2, Perley et al. (1979) find the velocity of electron flow along the jet to be ~ 1200 km s^{-1}.

However, there are a number of indications that this picture of a free jet may be oversimplified and not universally applicable.

First, the cone angles of some jets are not constant. For both NGC 315 (Bridle et al. 1979a) and 3C 449 (Perley et al. 1979), the jets shown in Figures 11 and 12, the cone angle initially decreases with distance, most of this "collimation" occurring within 30 kpc of the nucleus. This suggests that the beam can be influenced, perhaps even focused, by a circumgalactic medium. A further indication that jets may be affected by the galaxies through which they pass comes from 3C 83.1B/NGC 1265, the best-studied tailed radio galaxy (Miley et al. 1975, Owen et al. 1978a). Its jet, seen in Figure 14, has been observed to flare out about 10 kpc from the nucleus and this abrupt widening has been cited as evidence for the presence of a hot ($\sim 10^7$ K) dense ($\sim 10^{-2}$ cm^{-3}) interstellar medium in the central part of the elliptical galaxy (Owen et al. 1978a, Jones & Owen 1979).

Second, there are differences in the magnetic field configurations observed in various jets. Although in most jets in low luminosity radio galaxies the field is observed to be predominantly perpendicular to the jets, this may not be the case for high luminosity sources. In 3C 219, the only high luminosity source whose jet has been studied, the polarization distribution indicates a magnetic field aligned *along* the jet (Burch 1979b). Similarly, the bridges in most high luminosity sources have predominantly

parallel magnetic fields (e.g. Haves & Conway 1975, Miley 1976). It is unclear whether there is a distinction between a "bridge" in an edge-brightened double source and a "jet." The question of the magnetic field structure in jets is therefore complex. The interpretation is especially difficult because polarization position angles give merely the *projected* magnetic field directions. Fomalont et al. (1980) suggest that the three-dimensional field configuration in 3C 31 and NGC 315 may be helical.

Third, the surface brightness of the jet in 3C 31 decreases roughly as r^{-1}, compared with r^{-3} predicted by simple synchrotron theory (Valtonen 1979, Fomalont et al. 1979, Burch 1979c). Thus, to compensate for adiabatic losses there is likely to be an additional source of energy available to accelerate more particles or to amplify the field. As we have seen, even more stringent evidence for localized acceleration in jets is provided by the detection of optical emission.

Future searches for correlations between the radio and optical properties

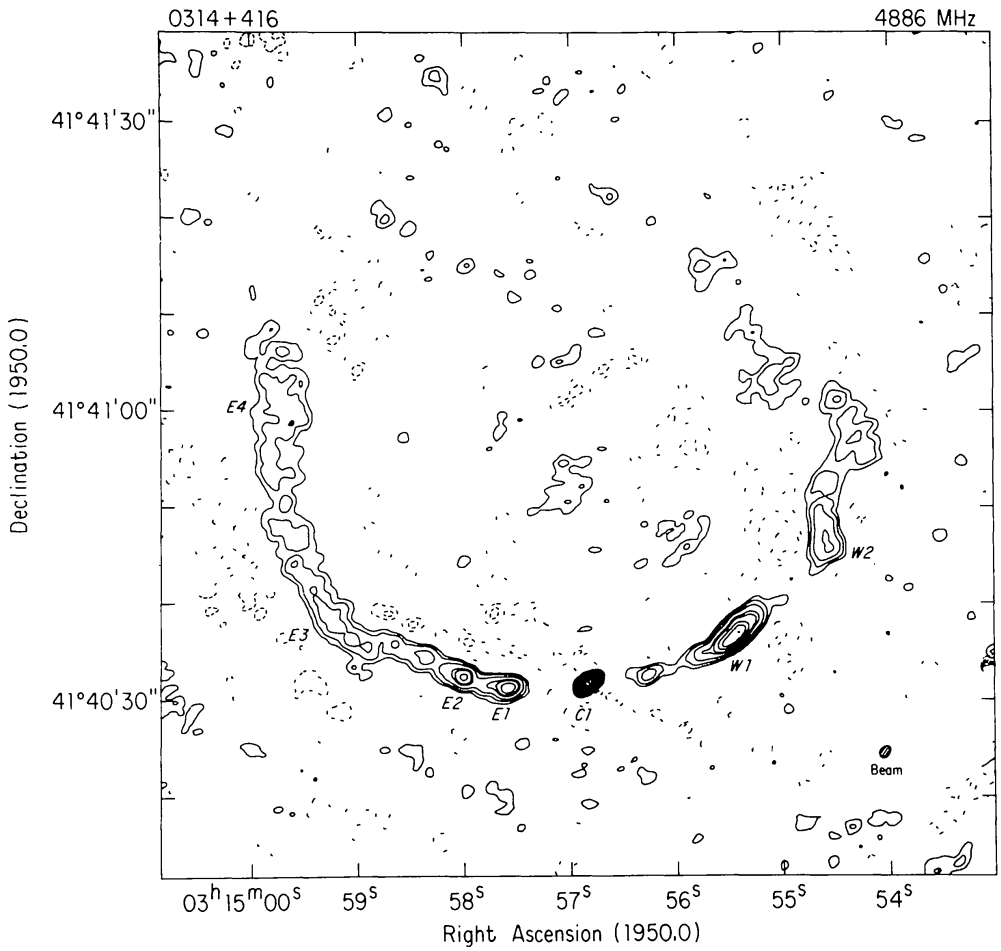

Figure 14 The head of the tailed source 3C 83.1B/NGC 1265 (VLA, 5 GHz) (from Owen et al. 1978a). See also Figure 8.

of jets and other radio-source parameters may help to elucidate the energy transport mechanism further.

The breakdown of a radio source into its elementary component parts has been useful in discussing the various processes involved, but it has inevitably been oversimplified. We have already remarked on the often arbitrary distinction between a "jet" and a "bridge." It is also not always possible to clearly distinguish between a "core" and a "jet." When the cores are observed with sufficient resolution jet-like structures are observed within them, e.g. the steep-spectrum core of Virgo A/M 87 (Figure 10) or the flat-spectrum core of NGC 6251 (Figure 9). The flat-spectrum cores, steep-spectrum cores, and jets are almost certainly all manifestations of different regimes in the energy transport process.

5 RADIO-SOURCE STRUCTURE AND THE ENVIRONMENT

> But it is an error to suppose, because we resolve to confine our attention to a certain number of the properties of an object that we therefore conceive, or have an idea of, the object denuded of its other properties.
>
> J. S. Mill, *Logics and Mathematics Based on Observation*

5.1 *Characteristic Scales*

Some typical scales observed in extended radio sources and their environment are compared in Table 2. Note the similarities between the characteristic radio and optical scales. These suggest that the radio-source phenomenon may be intimately connected with properties of the source environment. Here we shall consider possible relationships.

5.2 *Nuclear Activity*

Do the structures of extended radio sources identified with QSOs differ from those associated with galaxies? Although from the radio maps alone one cannot state with certainty whether an individual radio source is a

Table 2 Some characteristic scales observed in extended radio sources

Length (pc)	Radio	Optical
$\sim 10^{-3}$		Nuclear nonthermal continuum
$\sim 10^{-1}$	Flat-spectrum core	Broad (permitted) line region
$\sim 10^{3}$	Steep-spectrum core	Narrow (forbidden) line region
$\sim 10^{4.5}$		Galaxy
$\sim 10^{5.2}$	Extended radio source	Galactic halo

quasar or a radio galaxy there are several *statistical* differences between the two classes of objects.

As we saw in Section 2.1.1 quasars tend to have more pronounced hot spots and their structures are more asymmetric than sources associated with galaxies. However, because the radio luminosities of quasars are systematically larger than those of radio galaxies, it is impossible to state whether these effects are causally related to the nature of the parent optical objects or to the luminosity of the associated extended sources.

Nevertheless, a real difference is indicated by the fact that the radio cores of quasars are stronger than those of radio galaxies for sources that have extended emission of similar power. It seems reasonable to ascribe this difference to the existence of a correlation between the radio and optical core luminosities in extended radio sources. This is not a one-to-one relationship, however. Perhaps the optical core luminosity measures the instantaneous nuclear activity whereas the radio core represents the activity integrated over a longer period. A very likely possibility is that extended quasars are indeed radio galaxies undergoing transient active periods. The weak optical nonthermal emission seen in the nuclei of some radio galaxies (Yee & Oke 1978) could well be associated with the simmering remnant of a QSO. The more pronounced asymmetry between opposite lobes (Section 2.1.1) would then be a relativistic effect of orientation produced by a more energetic pumping of energy into the hot spots.

The most violent examples of ("present") nuclear activity are probably BL Lac objects. Although differences between their properties and those of quasars appear to be increasingly blurred, BL Lac objects are nominally characterized by high optical polarization, rapid variability at optical infrared and radio wavelengths, and weak or in most cases no observed emission lines. Until recently BL Lac objects were thought to possess little or no extended radio emission, but a survey by Weiler & Johnson (1980) has shown that 22 out of 42 objects surveyed have radio emission with sizes $\gtrsim 1''$. There is therefore no evidence that the properties of this emission are qualitatively different from those of extended radio emission in quasars and radio galaxies.

Emission lines in the parent nuclei of radio sources are strongly connected with their radio structure. Almost all extended quasars exhibit strong broad emission lines. The fraction is about half for the most luminous (edge-brightened-double) 3CR radio galaxies and only 10% for radio galaxies with $P_{178} \lesssim 10^{26}$ W Hz^{-1} (Hine & Longair 1979). For the limb-brightened double radio galaxies the ratio of core to extended flux increases with the width of the emission lines in a fairly continuous sequence from the extended radio galaxies to the extended quasars. This is

also consistent with models of radio sources in which a more active nucleus pumps more energy into the extended radio lobes.

Emission lines can also help differentiate quasars that possess extended radio structure from those that do not. A large proportion of all quasars have little or no associated extended structure; for a few of these, upper limits of $\sim 1\%$ have been set on the ratio of extended to compact structure at 610 MHz (Miley & Hartsuijker 1978). The QSOs with the broadest and most irregular emission lines seem to be associated with the extended radio sources, whereas those with relatively narrow emission lines have compact radio structures (Miley & Miller 1979). There is also a tendency for FeII emission lines to be found preferentially in quasars without extended radio structures (Setti & Woltjer 1977, Miley & Miller 1979). These relations, while not properly understood, indicate that the broad line emission regions are closely connected with the production of radio sources.

5.3 *Angles and Things*

All relations between the structure of radio sources and the properties of their associated galaxies and quasars give basic information concerning the formation of sources. During the last few years several statistical relationships have been discovered between gross optical features and radio structures.

One of the most important relations concerns the orientation of double radio sources relative to that of their parent galaxies. Recently, careful studies have been carried out to investigate this, with samples of 17 (Guthrie 1979) and 78 (Palimaka et al. 1979) objects respectively. In each case rigorous selection criteria were applied and only objects with accurately known radio and optical orientation were included. Both studies convincingly show (in contradiction to some earlier work, e.g. Gibson 1975, Sullivan & Sinn 1975) that the radio structures are preferentially but not exclusively aligned along the (projected) minor axes of the elliptical galaxies. This effect appears strongest for the largest radio sources, implying that alignment of the radio-source production axis with the parent galaxy minor axis may favor the development of giant radio sources.

If most radio galaxies rotate as nearly oblate systems, such an alignment would indicate that the radio-source axes are predominantly oriented along the angular momentum axes of the galaxies. The dynamics of five narrow edge-brightened double radio galaxies, 3C 33, 98, 184.1, 218, and Cygnus A have been studied (Simkin 1977, 1979) and in all cases the rotation axes of the gas and/or stars do seem indeed to be directed to within a few degrees of the radio structures.

Yet more evidence that the radio axis is related to the rotation axes of galaxies is provided by the dust lanes that are often seen to cross the optical

images of radio galaxies. A study of eight radio galaxies with dust lanes (Kotanyi & Ekers 1979, Kotanyi 1979, Ekers et al. 1978c) shows that the seven unambiguous cases have dust lanes perpendicular to the axes of the associated radio sources. But again this alignment is not exclusive (Butcher et al. 1980).

Alignment has also been observed between the extended radio structure and the optical polarization of QSOs. Most QSOs are weakly polarized at the 1% level or less. A comparison of the radio orientation and the optical polarization angles for 24 quasars shows that for 20 of them there is agreement to 30° (Stockman et al. 1979, Angel & Stockman 1980). Although the reason for this alignment is unknown, one can draw the elementary conclusion that the long term memory of direction established for edge-brightened double radio galaxies is also a feature of edge-brightened double quasars.

The apparently simple dynamical behavior of galaxies associated with edge-brightened double sources contrasts with the disturbed optical appearance and complex spectroscopic properties of the few wide extended radio galaxies whose distributions have been studied spectroscopically — e.g. NGC 5128/Centaurus A (Blanco et al. 1975, Osmer 1978, Dufour et al. 1979, Graham 1979), NGC 1316/Fornax A (Schweizer 1979), M87/Virgo A (Young et al. 1978, Sargent et al. 1978), and NGC 1275/3C 84 (Burbidge & Burbidge 1965, Rubin et al. 1977). In both Fornax A and Centaurus A, disks of gas and dust are misaligned with the major stellar axes and it has been suggested that the optical properties of these giant elliptical galaxies have been affected by merging. A connection between wide radio sources and galaxy merging would be consistent with Rees's (1978b) suggestion (Section 2.2.3) that merging can cause misalignment between the angular momentum axis of a galaxy and of the nuclear machine responsible for radio emission. The radio ejection axis would then precess, causing a wide radio source to be produced with a wide rotationally symmetric morphology. It may be significant that in Centaurus A the dust lane (Graham 1979) is warped in the same sense as the extended radio emission (Cooper et al. 1965).

Finally, we mention another possible connection between radio and optical morphology which could, if confirmed, be profoundly important. Some years ago it was discovered that two of the brightest tailed radio galaxies, NGC 1265/3C 83.1B and NGC 7720/3C 465, have asymmetric optical brightness distribution, both having the steepest gradients in the direction of their radio heads (Bertola & Perola 1973). On the radio-trail picture this might imply the existence of a relation between the optical asymmetry and the direction of motion of a galaxy in a rich cluster. Since this effect was reported, the sample of tailed radio galaxies has been

enlarged considerably and work is at present in progress to investigate whether there is indeed a statistically significant relation between optical asymmetry and radio morphology (E. A. Valentijn et al., in preparation).

5.4 *Clustering of Galaxies*

In recent years there have been several studies on the effect of cluster membership on the structure of radio galaxies. There is general agreement that sources inside clusters have more complex structures than those outside (Lari & Perola 1977, Rudnick & Owen 1977, Burns & Owen 1977, Simon 1978, McHardy 1979). The more bent sources have a larger density of galaxies surrounding them (Stocke 1979) and of the 26 narrow-tailed sources catalogued by Valentijn (1979b) all except two occur in rich clusters. Three narrow-tailed sources occur in the Perseus Cluster (Gisler & Miley 1979) and five others in Abell 2256 (Bridle & Fomalont 1976, Bridle

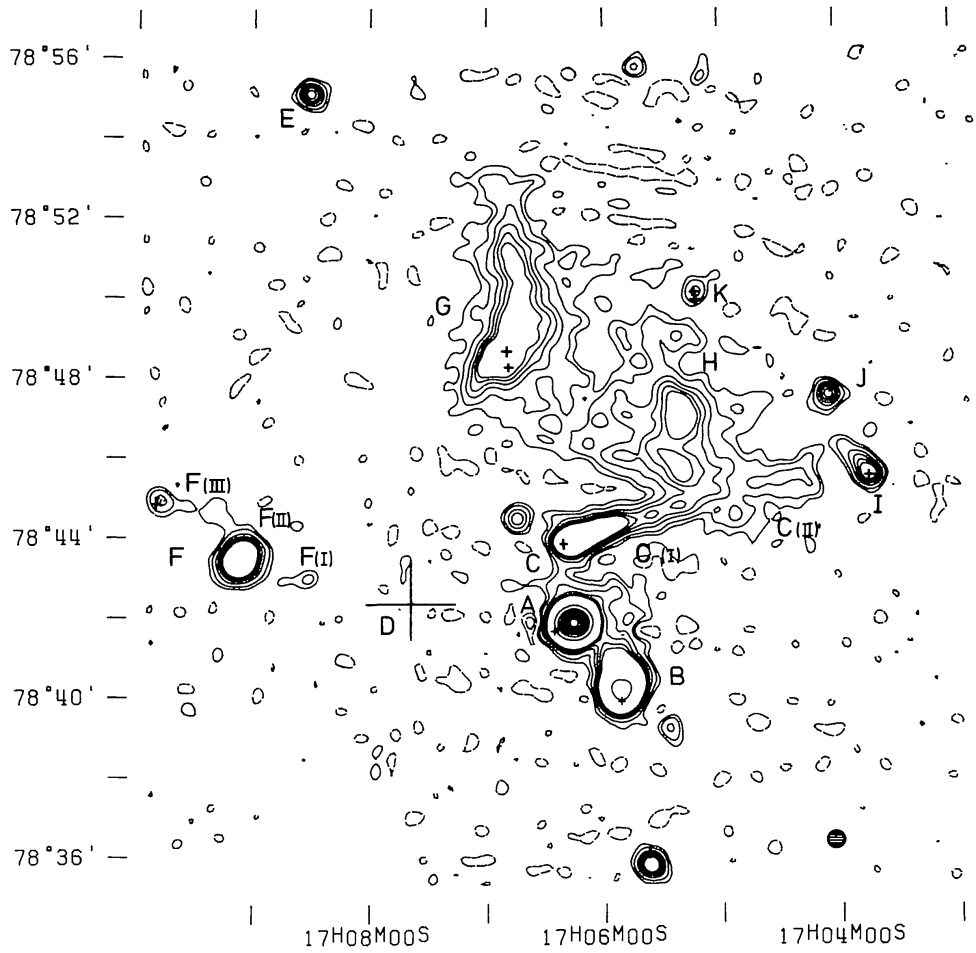

Figure 15 Intensity contours of 1.4-GHz emission from the cluster Abell 2256 (Westerbork). The crosses mark the positions of associated galaxies. The cluster contains at least 4 and possibly 8 tailed radio galaxies (from Bridle et al. 1979b).

et al. 1979b). Both these clusters have large intrinsic X-ray powers and their galaxies have high radial velocity dispersions. Dynamically active clusters containing dense hot gas are therefore good spawning grounds for tailed sources, as would be expected from the radio-trail hypothesis (Section 2.2.1).

Because of the preferential occurrence of distorted radio galaxy morphologies in rich clusters it has been suggested that quasars with bent structures may be suitable indicators of X-ray clusters at intermediate and high redshifts (Hintzen & Scott 1978).

In Section 2.2.1 we saw that more highly bent radio sources tend to have optically fainter parent galaxies. Another form in which this correlation manifests itself is the fact that radio sources associated with dominant cluster galaxies tend to be only slightly bent, whereas the narrow-tailed sources tend to be associated with nondominant galaxies (Rudnick & Owen 1977, McHardy 1979, Simon 1978, Valentijn 1979b).

If an intergalactic medium plays a role in confining radio sources, one might well expect the physical sizes of sources to be smaller inside clusters, where the medium is probably denser and hotter. Whether cluster membership influences radio-source sizes is still controversial. McHardy (1979) finds that 4C sources in Abell clusters are not significantly larger than field sources. On the other hand Stocke (1979) and Guindon (1979) concluded that source sizes are systematically larger in regions of low galactic density. In both the latter studies the density of galaxies was determined in the vicinity of strong radio galaxies.

6 CONCLUSIONS

> Life is the art of drawing conclusions from insufficient premises.
>
> Samuel Butler, *Notebooks*

The enormous amount of structural data gathered in recent years suggests the following description of the radio-source phenomenon. A "machine" imbedded in the nucleus of a galaxy ejects a collimated flux of energy in two opposite directions along its angular momentum axis (Section 4.3.3) in the form of a recurrent spluttering of plasmons or a quasi-continuous "beam" of relativistic particles. As a fairly direct manifestation of this nuclear activity we see radio and optical ("quasar") continuum cores and broad line emission regions (Sections 4.3 and 5.2). Provided the nuclear activity is strong enough, prolonged enough, and/or stable enough in direction, an extended radio source is built up. The overall morphology of the extended lobes is determined by the degree of activity, as well as the amount of

translational and/or rotational motion of the nuclear machine and/or of the surrounding medium (Sections 2.2, 3 and 4).

What is the nuclear machine? There are several pointers that it may be a rotating black hole that derives its energy from accretion (Lynden-Bell 1969). First, one can cite the elephantine memory for direction discussed in Sections 4.3 and 5.2. Second, photometric and spectroscopic studies of M 87 provide some direct evidence for the presence of a black hole in this, one of the closest radio galaxies (Sargent et al. 1978, Young et al. 1978). Third, collimated extragalactic radio sources have several properties in common with the nonthermal radio emission associated with some galactic X-ray stars (e.g. Braes & Miley 1973). For example the triple source associated with Sco X-1 is uncannily like a miniature edge-brightened extragalactic radio source. SS 433 also shows extended radio emission symmetrically distributed with respect to an X-ray star (Spencer 1979; W. Gilmore and E. R. Seaquist, in preparation; R. Hjellming, K. J. Johnson, and G. K. Miley, in preparation). The only energy sources that have been put forward as possible power houses for both X-ray stars and galactic nuclei are accreting black holes. Fourth, the energy budget is consistent with the appetite of a not too hungry black hole. The most energetic radio sources require total energies in excess of 10^{60} ergs supplied over a period probably longer than 10^8 yr (an age derived by combining the most plausible outflow speeds in Section 4.4 with the typical source sizes for Section 2.3). The resultant energy needs of $\gtrsim 10^{-2}\, M_\odot$ per year could well be supplied by an accreting black hole buried in a dense galactic nucleus.

Although the above scenario is certainly very oversimplified and possibly conceptually wrong, it is, in my view, the most plausible unified picture consistent with currently available data.

In the near future we shall certainly see further progress on the observational side. The completed VLA will map the detailed morphologies of the jets and hot spots, while more sophisticated optical detectors will provide visual information. The resultant statistical studies should enlarge our knowledge of the energy transport and particle acceleration processes. Second, and perhaps more important, there is the possibility of tackling one of the most intriguing remaining problems—the nature of the nuclear energy conversion and collimation processes. There must be a fundamental mechanism which works over a vast range of physical conditions which can produce collimated radio sources with sizes spanning more than a factor of 10^7 and energies more than a factor of 10^{20}. During the next few years we may expect to see an attack on this problem from several separate wavelength regions. More sensitive VLBI measurements of radio cores of both galactic and extragalactic sources will become available together with the Einstein Observatory's X-ray data. In addition high

resolution optical observations from the space telescope should provide considerable information about the dynamics of the inner regions of active galaxies. A third fruitful avenue of research promises to be a continuation of the work described in Section 5.3, carrying out more detailed comparisons between the morphologies of radio sources and the structures and dynamics of their parent galaxies.

Nearly three decades ago an historic encounter took place in which Baade wagered Minkowski a bottle of premium whisky that the visible object identified with Cygnus A was a colliding pair of galaxies. Baade apparently lost the bet. More recently it has been suggested that the hypothetical nuclear black holes that power extended extragalactic radio sources are fueled by infall of material to the nuclei (see, for example, Rees 1978b). The rate of infall may well be influenced by galaxy merging, a process now thought to play an important role in the evolution of galaxies (e.g. Silk & Norman 1979). It is ironic that the wheel of theory shows signs of moving almost full circle. Surely Baade posthumously deserves at least half a bottle of medium quality whisky?

ACKNOWLEDGMENTS

Review articles inevitably reflect the personal preferences and prejudices of the author. I am grateful to the many friends and colleagues who over the years were instrumental in forming my present conditioned outlook. Without risk of incrimination I also wish to thank Wil van Breugel, Ed Fomalont, Dan Harris, Harry van der Laan, Colin Norman, Richard Strom, Tony Willis, and Lorenzo Zaninetti for critically reading the manuscript and Lenore for patiently typing it. I acknowledge the receipt of a NATO research grant (no. 1828).

Literature Cited

Allen, L. R., Hanbury Brown, R., Palmer, H. P. 1963. *MNRAS* 125:57
Andernach, H., Baker, J. R., von Kap-herr, A., Wielebinski, R. 1979. *Astron. Astrophys.* 74:93
Angel, J. R. P., Stockman, H. S. 1980. *Ann. Rev. Astron. Astrophys.* 18:321
Argue, A. N., Riley, J. M., Pooley, G. G. 1978. *Observatory* 98:132
Auriemma, C., Perola, G. C., Ekers, R., Fanti, R., Lari, C., Jaffe, W. J., Ulrich, M. H. 1977. *Astron. Astrophys.* 57:41
Baade, W. 1956. *Ap. J.* 123:550
Baggio, R., Perola, G. C. Tarenghi, M. 1978. *Astron. Astrophys.* 70:303
Baldwin, J. E., Scott, P. F. 1973. *MNRAS* 165:259
Barber, D., Donaldson, W., Miley, G. K., Smith, H. 1966. *Nature* 209:753
Bare, C., Clark, B. G., Kellermann, K. I., Cohen, M. H., Jauncey, D. L. 1967. *Science* 157:189
Benford, G. 1979. *MNRAS* 183:29
Berlin, A. B., Gol'nev, V. Ya., Esepkina, N. A., Zverev, Yu. K., Ipatov, A. V., Kaidanovskii, N. L., Korol'kov, D. V., Lavrov, A. P., Pariiskii, Yu. N., Soboleva, N. S., Stotskii, A. A., Timofeeva, G. M., Shivris, O. N. 1975. *Sov. Astron. Lett.* 1:234, *Pis'ma Astron. Zh.* 1:3

Bertola, F., Perola, G. C. 1973. *Astrophys. Lett.* 14:7
Birkinshaw, M. 1980. *MNRAS* 190:793
Birkinshaw, M., Laing, R., Scheuer, P., Simon, A. 1978. *MNRAS* 185:39P
Blanco, V. M., Graham, J. A., Lasker, B. M., Osmer, P. S. 1975. *Ap. J. Lett.* 198:L63
Blandford, R. D. 1976. *MNRAS* 176:465
Blandford, R. D., Icke, V. 1978. *MNRAS* 185:527
Blandford, R. D., Königl, A. 1979. *Astrophys. Lett.* 20:15
Blandford, R. D., Ostriker, J. P. 1978. *Ap. J. Lett.* 221:L29
Blandford, R. D., Pringle, J. E. 1976. *MNRAS* 176:443
Blandford, R. D., Rees, M. J. 1974. *MNRAS* 169:395
Blandford, R. D., Rees, M. J. 1978. *Physica Scripta* 17:265
Blumenthal, G., Miley, G. K. 1979. *Astron. Astrophys.* 80:13
Braes, L. L. E., Miley, G. K. 1973. *Proc. IAU Symp. 55, X-Ray and Gamma-Ray Astronomy*, p. 86
Bridle, A. H., Feldman, P. A. 1972. *Nature Phys. Sci.* 235:168
Bridle, A. H., Fomalont, E. B. 1976. *Astron. Astrophys.* 52:107
Bridle, A. H., Fomalont, E. B. 1978. *Astron. J.* 83:704
Bridle, A. H., Davis, M. M., Meloy, D. A., Fomalont, E. B., Strom, R. G., Willis, A. G. 1976. *Nature* 262:179
Bridle, A. H., Davis, M. M., Fomalont, E. B., Willis, A. G., Strom, R. G. 1979a. *Ap. J. Lett.* 228:L9
Bridle, A. H., Fomalont, E. B., Miley, G. K., Valentijn, E. A. 1979b. *Astron. Astrophys.* 80:201
Broten, N. W., Clarke, R. W., Legg, T. H., Locke, J. L., McLeish, C. W., Richards, R. S., Yen, J. L., Chisholm, R. M., Galt, J. A. 1967. *Nature* 216:44
Brown, R. H., Palmer, H. P., Thompson, A. R. 1955. *Philos. Mag.* 46:857
Burbidge, E. M., Burbidge, G. R. 1965. *Ap. J.* 142:1351
Burbidge, E. M., Smith, H. E., Burbidge, G. R. 1975. *Ap. J. Lett.* 199:L137
Burbidge, E. M., Smith, H. E., Burbidge, G. R. 1978. *Ap. J.* 219:400
Burbidge, G. R. 1967. *Nature* 216:1287
Burch, S. F. 1977a. *MNRAS* 180:623
Burch, S. F. 1977b. *MNRAS* 181:599
Burch, S. F. 1979a. *MNRAS* 186:293
Burch, S. F. 1979b. *MNRAS* 186:519
Burch, S. F. 1979c. *MNRAS* 187:187
Burn, B. J. 1966. *MNRAS* 133:67
Burns, J. O., Owen, F. N. 1977. *Ap. J.* 217:34
Butcher, H., van Breugel, W. J. M., Miley, G. K. 1980. *Ap. J.* 235:749
Byrd, G. G., Valtonen, M. J. 1978. *Ap. J.* 221:481
Bystedt, J., Högbom, J. A. 1979. Preprint submitted to *Nature*
Callahan, P. S. 1976. *MNRAS* 174:587
Cameron, M. J. 1971. *MNRAS* 152:439
Catura, R. C., Fischer, P. C., Johnson, H. M., Meyerott, A. J. 1972. *Ap. J. Lett.* 177:L1
Christiansen, W. A. 1969. *MNRAS* 145:327
Christiansen, W. A., Pacholczyk, A. G., Scott, J. S. 1977. *Nature* 266:593
Christiansen, W. N., Frater, R. H., Watkinson, A., O'Sullivan, J. D., Lockhart, I. A., Goss, W. M. 1977. *MNRAS* 181:183
Cohen, M. H. 1969. *Ann. Rev. Astron. Astrophys.* 7:619
Cohen, M. H., Readhead, A. C. S. 1979. *Ap. J. Lett.* 233:L101
Cohen, M. H., Gundermann, E. J., Harris, D. E. 1967. *Ap. J.* 150:767
Conway, R. G., Kronberg, P. P. 1969. *MNRAS* 142:11
Conway, R. G., Stannard, D. 1975. *Nature* 255:310
Cooke, B. A., Lawrence, A., Perola, G. C. 1978. *MNRAS* 182:661
Cooper, B. F. C., Price, R. M., Cole, D. J. 1965. *Aust. J. Phys.* 18:589
Costain, C. H., Bridle, A. H., Feldman, P. A. 1972. *Ap. J. Lett.* 175:L15
Cowie, L. L., McKee, C. F. 1975. *Astron. Astrophys.* 43:337
Crane, P. C. 1979. *Astron. J.* 84:281
Curtis, H. D. 1918. *Lick Obs. Publ.* 13:11
Davis, R. J., Stannard, D., Conway, R. G. 1977. *Nature* 267:596
Davis, R. J., Stannard, D., Conway, R. G. 1978. *MNRAS* 185:453
de Bruyn, A. G. 1978. *Proc. IAU Symp. 77, The Structure and Properties of Nearby Galaxies*, p. 205
de Bruyn, A. G., Wilson, A. S. 1978. *Astron. Astrophys.* 64:433
Dent, W. A., Haddock, F. T. 1965. *Nature* 205:487
de Vaucouleurs, G., Angione, R., Fraser, C. W. 1968. *Astrophys. Lett.* 2:141
De Young, D. S. 1976. *Ann. Rev. Astron. Astrophys.* 14:447
De Young, D. S., Axford, W. I. 1967. *Nature* 216:129
De Young, D. S., Hogg, D. E., Wilkes, C. T. 1979. *Ap. J.* 228:43
Downes, A. 1980. *MNRAS* 190:261
Dreher, J. W. 1979. *Ap. J.* 230:687
Dufour, R. J., van den Bergh, S. 1978. *Ap. J. Lett.* 226:L73
Dufour, R. J., van den Bergh, S., Harvel, C. A., Martins, D. H., Schiffer, F. H. III, Talbot, R. J. Jr., Talent, D. L., Wells, D. C. 1979. *Astron. J.* 84:284
Eichler, D. 1979. *Ap. J.* 229:419

Eilek, J. A. 1979. *Ap. J.* 230:373
Ekers, R. D. 1978. *Proc. IAU Symp. 77, The Structure and Properties of Nearby Galaxies*, p. 221
Ekers, R. D., Miley, G. K. 1977. *Proc. IAU Symp. 74*, p. 109
Ekers, R. D., Fanti, R., Lari, C., Parma, P. 1978a. *Nature* 276:588
Ekers, R. D., Fanti, R., Lari, C., Ulrich, M.-H. 1978b. *Astron. Astrophys.* 69:253
Ekers, R. D., Goss, W. M., Kotanyi, C. G., Skellern, D. J. 1978c. *Astron. Astrophys.* 69:L21
Elgaroy, O., Morris, D., Rowson, B. 1962. *MNRAS* 124:395
Emerson, D. T., Klein, U., Haslam, C. G. T. 1979. *Astron. Astrophys.* 76:92
Fabbiano, G., Doxsey, R. E., Johnston, M., Schwartz, D. A., Schwarz, J. 1979. *Ap. J. Lett.* 230:L67
Fanaroff, B. L., Riley, J. M. 1974. *MNRAS* 167:31p
Fanti, R., Perola, G. C. 1977. *Proc. IAU Symp. 74*, p. 171
Ferrari, A., Trussoni, E., Zaninetti, L. 1979. *Astron. Astrophys.* 79:190
Flasar, F. M., Morrison, P. 1976. *Ap. J.* 204:352
Fomalont, E. B. 1969. *Ap. J.* 157:1027
Fomalont, E. B. 1972. *Astrophys. Lett.* 12:187
Fomalont, E. B. 1979. *IAU Comm. 40 Rep.*, ed. H. van der Laan. *IAU Trans.* 17A(3):149
Fomalont, E. B., Miley, G. K. 1975. *Nature* 257:99
Fomalont, E. B., Wright, M. C. H. 1974. *Galactic and Extragalactic Radio Astronomy*, chap. 10, ed. G. L. Verschuur, K. I. Kellermann. Berlin: Springer
Fomalont, E. B., Miley, G. K., Bridle, A. H. 1979. *Astron. Astrophys.* 76:106
Fomalont, E. B., Bridle, A. H., Willis, A. G., Perley, R. A. 1980. Preprint
Forster, J. R. 1980. *Ap. J.* In press
Forster, J. R., Dreher, J., Wright, M. C. H., Welch, W. J. 1978. *Ap. J. Lett.* 221:L3
Gardner, F. F., Whiteoak, J. B. 1966. *Ann. Rev. Astron. Astrophys.* 4:245
Gavazzi, G. 1978. *Astron. Astrophys.* 69:355
Gavazzi, G., Perola, G. C. 1978. *Astron. Astrophys.* 66:407
Geldzahler, B. J., Fomalont, E. B. 1978. *Astron. J.* 83:1047
Getmansev, G. G., Ginzburg, V. L. 1950. *Zh. Eksp. Teor. Fiz.* 20:347
Ghigo, F. D. 1978. *Astron. J.* 83:1363
Gibson, D. M. 1975. *Astron. Astrophys.* 39:377
Gisler, G. R., Miley, G. K. 1979. *Astron. Astrophys.* 76:109
Gopal-Krishna. 1977. *MNRAS* 181:247
Gopal-Krishna, Swarup, G. 1977. *MNRAS* 178:265
Goss, W. M., Wellington, K. J., Christiansen, W. N., Lockhart, I. A., Watkinson, A., Frater, R. H., Little, A. G. 1977. *MNRAS* 178:525
Graham, J. A. 1979. *Ap. J.* 232:60
Guindon, B. 1979. *MNRAS* 186:117
Gursky, H., Schwartz, D. A. 1977. *Ann. Rev. Astron. Astrophys.* 15:541
Guthrie, B. N. G. 1979. *MNRAS* 187:581
Hanisch, R. J., Matthews, T. A., Davis, M. M. 1979. *Astron. J.* 84:946
Hargrave, P. J., McEllin, M. 1975. *MNRAS* 173:37
Hargrave, P. J., Ryle, M. 1974. *MNRAS* 166:305
Hargrave, P. J., Ryle, M. 1976. *MNRAS* 175:481
Harris, A. 1974. *MNRAS* 166:449
Harris, D. E., Grindlay, J. E. 1979. *MNRAS* 188:25
Harris, D. E., Miley, G. K. 1978. *Astron. Astrophys. Suppl.* 34:117
Harris, D. E., Romanishin, W. 1974. *Ap. J.* 188:209
Harris, D. E., Kapahi, V. K., Ekers, R. D. 1980. *Astron. Astrophys. Suppl.* 39:215
Haves, P. 1975. *MNRAS* 173:553
Haves, P., Conway, R. G. 1975. *MNRAS* 173:53p
Hazard, C., Mackey, M. B., Shimmins, A. J. 1963. *Nature* 197:1037
Hewish, A., Scott, P. F., Wills, D. 1964. *Nature* 203:1214
Hill, J. M., Longair, M. S. 1971. *MNRAS* 154:125
Hiltner, W. A. 1959. *Ap. J.* 130:340
Hine, R. G., Longair, M. S. 1979. *MNRAS* 188:111
Hintzen, P., Scott, J. S. 1978. *Ap. J. Lett.* 224:L47
Hintzen, P., Scott, J. S., Tarenghi, M. 1977. *Ap. J.* 212:8
Högbom, J. A. 1974. *Astron. Astrophys. Suppl.* 15:417
Högbom, J. A. 1979. *Astron. Astrophys. Suppl.* 36:173
Hogg, D. E., Macdonald, G. H., Conway, R. G., Wade, C. M. 1969. *Astron. J.* 74:1206
Holman, G. D., Ionson, J. A., Scott, J. S. 1979. *Ap. J.* 228:576
Ingham, W., Morrison, P. 1975. *MNRAS* 173:569
Jaffe, W. J. 1977. *Ap. J.* 212:1
Jaffe, W. J., Perola, G. C. 1973. *Astron. Astrophys.* 26:423
Jaffe, W. J., Rudnick, L. 1979. *Ap. J.* 233:453
Jaffe, W. J., Perola, G. C., Valentijn, E. A. 1976. *Astron. Astrophys.* 49:179

Jenkins, C. J., McEllin, M. 1977. *MNRAS* 180:219
Jenkins, C. J., Scheuer, P. A. G. 1976. *MNRAS* 174:327
Jenkins, C. J., Pooley, G. G., Riley, J. M. 1977. *Mem. RAS* 84:61
Jennison, R. C. 1958. *MNRAS* 118:276
Jennison, R. C., Das Gupta, M. K. 1953. *Nature* 172:996
Jones, T. W., Owen, F. N. 1979. *Ap. J.* 234:818
Joshi, M. N., Gopal-Krishna. 1977. *MNRAS* 178:717
Kapahi, V. K. 1975. *MNRAS* 172:513
Kapahi, V. K. 1978. *Astron. Astrophys.* 67:157
Kapahi, V. K., Schilizzi, R. T. 1979. *Nature* 277:610
Katgert-Merkelijn, J., Lari, C., Padrielli, L. 1980. *Astron. Astrophys. Suppl.* 40:91
Kellermann, K. I. 1978. *Physica Scripta* 17:257
Kellermann, K. I., Clark, B. G., Niell, A. E., Shaffer, D. B. 1975. *Ap. J.* 197:L113
Kellermann, K. I., Shaffer, D. B., Purcell, G. H., Pauliny-Toth, I. I. K., Preuss, E., Witzel, A., Graham, D., Schilizzi, R. T., Cohen, M. H., Moffet, A. T., Romney, J. D., Niell, A. E. 1977. *Ap. J.* 211:658
Kotanyi, C. G. 1979. *Astron. Astrophys.* 74:156
Kotanyi, C. G., Ekers, R. D. 1979. *Astron. Astrophys.* 73:L1
Kronberg, P. P., Strom, R. G. 1977. *Ap. J.* 215:438
Lacombe, C. 1977. *Astron. Astrophys.* 54:1
Lari, C., Perola, G. C. 1977. *Proc. IAU Symp. 79, The Large Scale Structure of the Universe*, p. 137
Little, L. T., Hewish, A. 1968. *MNRAS* 138:393
Longair, M. S., Riley, J. M. 1979. *MNRAS* 188:625
Longair, M. S., Ryle, M., Scheuer, P. A. G. 1973. *MNRAS* 164:243
Lovelace, R. V. E. 1976. *Nature* 262:649
Lynden-Bell, D. 1969. *Nature* 223:690
Macdonald, G. H., Kenderdine, S., Neville, A. C. 1968. *MNRAS* 138:259
Mackay, C. D. 1971. *MNRAS* 154:209
Maltby, P., Moffet, A. T. 1963. *Ap. J. Suppl.* 7:141
Masson, C. R. 1979. *MNRAS* 187:253
Masson, C. R., Mayer, C. J. 1978. *MNRAS* 185:607
McHardy, I. M. 1979. *MNRAS* 188:495
McVittie, G. C. 1965. *General Relativity and Cosmology*. London: Chapman & Hall. 2nd ed.
Miley, G. K. 1971. *MNRAS* 152:477
Miley, G. K. 1973. *Astron. Astrophys.* 26:413
Miley, G. K. 1974. *Proc. IAU Symp. 58, Formation and Dynamics of Galaxies*, p. 109
Miley, G. K. 1976, *Proc. NATO Summer School, Physics of Non-Thermal Radio Sources*, p. 1, Dordrecht: Reidel
Miley, G. K., Harris, D. E. 1977. *Astron. Astrophys.* 61:L23
Miley, G. K., Hartsuijker, A. P. 1978. *Astron. Astrophys. Suppl.* 34:129
Miley, G. K., Miller, J. M. 1979. *Ap. J. Lett.* 228:L55
Miley, G. K., Perola, G. C. 1975. *Astron. Astrophys.* 45:223
Miley, G. K., van der Laan, H. 1973. *Astron. Astrophys.* 28:359
Miley, G. K., Wade, C. M. 1971. *Astrophys. Lett.* 8:11
Miley, G. K., Perola, G. C., van der Kruit, P. C., van der Laan, H. 1972. *Nature* 237:269
Miley, G. K., Wellington, K. J., van der Laan, H. 1975. *Astron. Astrophys.* 38:381
Miley, G. K., Wellington, K. J., van der Laan, H. 1975. *Astron. Astrophys.* 38:381
Mills, D. M., Sturrock, P. A. 1970. *Astrophys. Lett.* 5:105
Mitton, S. 1970. *Astrophys. Lett.* 6:161
Moffet, A. T. 1966. *Ann. Rev. Astron. Astrophys.* 4:145
Moffet, A. T. 1975. *Stars and Stellar Systems*, Vol. IX, p. 211. Univ. Chicago Press
Moffet, A. T. 1979. *IAU Comm. 40 Rep.*, ed. H. van der Laan. *IAU Trans.* 17A(3):155
Mushotzky, R. F., Serlemittos, P. J., Smith, B. W., Boldt, E. A., Holt, S. S. 1978. *Ap. J.* 255:21
Norman, C., Silk, J. 1979. *Ap. J. Lett.* 233:L1
Northover, K. J. E. 1976. *MNRAS* 177:307
Oort, J. H. 1977. *Ann. Rev. Astron. Astrophys.* 15:295
Osmer, P. S. 1978. *Ap. J. Lett.* 226:L79
Owen, F. N., Rudnick, L. 1976. *Ap. J. Lett.* 205:L1
Owen, F. N., Burns, J. O., Rudnick, L. 1978a. *Ap. J. Lett.* 226:L119
Owen, F. N., Porcas, R. W., Neff, S. G. 1978b. *Astron. J.* 83:1009
Owen, F. N., Burns, J. O., Rudnick, L., Greisen, E. W. 1979. *Ap. J. Lett.* 229:L59
Pacholczyk, A. G. 1970. *Radio Astrophysics*, Chap. 7. San Francisco: Freeman
Pacholczyk, A. G. 1977. *Radio Galaxies*, Chap. 5. Oxford: Pergamon
Pacholczyk, A. G., Scott, J. S. 1976. *Ap. J.* 203:313
Palimaka, J. J., Bridle, A. H., Fomalont, E. B., Brandie, G. W. 1979. *Ap. J. Lett.* 231:L7
Palmer, H. P., Rowson, B., Anderson, B., Donaldson, W., Miley, G. K., Gent, H., Adgie, R. L., Slee, O. B., Crowther, J. H. 1967. *Nature* 213:789
Pauliny-Toth, I. I. K., Preuss, E., Witzel, A.,

Kellermann, K. I., Shaffer, D. B. 1976. *Astron. Astrophys.* 52:471
Perley, R. A., Johnston, K. J. 1979. *Astron. J.* 84:1247
Perley, R. A., Willis, A. G., Scott, J. S. 1979. *Nature* 281:437
Perola, G. C., Reinhardt, M. 1972. *Astron. Astrophys.* 17:432
Pooley, G. G., Henbest, S. N. 1974. *MNRAS* 169:477
Potash, R. I., Wardle, J. F. C. 1979. *Astron. J.* 84:707
Potash, R. I., Wardle, J. F. C. 1980. Preprint
Readhead, A. C. S., Hewish, A. 1976. *MNRAS* 1976:571
Readhead, A. C. S., Wilkinson, P. N. 1978. *Ap. J.* 223:25
Readhead, A. C. S., Cohen, M. H., Pearson, T. J., Wilkinson, P. N. 1978a. *Nature* 276:768
Readhead, A. C. S., Cohen, M. H., Blandford, R. D. 1978b. *Nature* 272:131
Readhead, A. C. S., Pearson, T. J., Cohen, M. H., Ewing, M. S., Moffet, A. T. 1979. *Ap. J.* 231:299
Rees, M. J. 1971. *Nature* 229:312, 510
Rees, M. J. 1978a. *MNRAS* 184:61p
Rees, M. J. 1978b. *Nature* 275:516
Reich, W., Kalberla, P., Reif, K., Neidhöfer, J. 1978. *Astron. Astrophys.* 69:165
Riley, J. M., Jenkins, C. J. 1977. *Proc. IAU Symp. 74, Radio Astronomy and Cosmology*, p. 237
Riley, J. M., Pooley, G. G. 1975. *Mem. RAS* 80:93
Riley, J. M., Pooley, G. G. 1978. *MNRAS* 183:245
Rubin, V. C., Ford, W. K., Peterson, C. J., Oort, J. H. 1977. *Ap. J.* 211:693
Rudnick, L., Owen, F. N. 1977. *Astron. J.* 82:1
Ryle, M., Hewish, A. 1960. *MNRAS* 120:220
Ryle, M., Vonberg, D. D. 1948. *Proc. R. Soc. London Ser. A.* 193:98
Ryle, M., Windram, M. D. 1968. *MNRAS* 138:1
Sargent, W. L. W., Young, P. J., Boksenberg, A., Shortridge, K., Lynds, C. R., Hartwick, F. D. A. 1978. *Ap. J.* 221:731
Saslaw, W. C., Valtonen, M. J., Aarseth, S. J. 1974. *Ap. J.* 190:253
Saslaw, W. C., Tyson, J., Crane, P. 1978. *Ap. J.* 222:435
Scheuer, P. A. G. 1962. *Aust. J. Phys.* 15:333
Scheuer, P. A. G. 1974. *MNRAS* 166:513
Scheuer, P. A. G., Readhead, A. C. S. 1979. *Nature* 277:182
Schilizzi, R. T., Ekers, R. D. 1975. *Astron. Astrophys.* 40:221
Schilizzi, R. T., Miley, G. K., van Ardenne, A., Baud, B., Baath, L., Rönnäng, B. O., Pauliny-Toth, I. I. K. 1979. *Astron. Astrophys.* 77:1
Schmidt, G. D., Peterson, B. M., Beaver, E. A. 1978. *Ap. J. Lett.* 220:L31
Schreier, E. J., Feigelson, E., Delvaille, J., Giacconi, R., Grindlay, J., Schwartz, D. A., Fabian, A. C. 1980. *Ap. J. Lett.* 234:L39
Schwartz, U. J. 1978. *Astron. Astrophys.* 65:345
Schweizer, F. 1979. Preprint
Setti, G., Woltjer, L. 1977. *Ap. J. Lett.* 218:L33
Silk, J., Norman, C. A. 1979. *Ap. J.* 234:86
Simkin, S. M. 1977. *Ap. J.* 217:45
Simkin, S. M. 1978. *Ap. J. Lett.* 222:L55
Simkin, S. M. 1979. *Ap. J.* 234:56
Simkin, S. M., Ekers, R. D. 1979. *Astron. J.* 84:56
Simon, A. J. B. 1978. *MNRAS* 184:537
Simon, A. J. B. 1979. *MNRAS* 188:637
Slingo, A. 1974. *MNRAS* 168:307
Smith, M. D., Norman, C. A. 1979. *Astron. Astrophys.* 81:282
Spangler, S. R. 1979. *Ap. J. Lett.* 232:L7
Spangler, S. R., Meyers, K. A. 1978. *Astron. J.* 83:547
Speed, B., Warwick, R. S. 1978. *MNRAS* 182:761
Spencer, R. E. 1979. *Nature* 282:482
Stannard, D., Neal, D. S. 1977. *MNRAS* 179:719
Stocke, J. 1979. *Ap. J.* 230:40
Stockman, H. S., Angel, J. R. P., Miley, G. K. 1979. *Ap. J. Lett.* 227:L55
Strom, R. G., Willis, A. G. 1979. *Astron. Astrophys.* In press
Strom, R. G., Willis, A. G., Wilson, A. S. 1978. *Astron. Astrophys.* 68:367
Sullivan, W. T. III., Sinn, L. A. 1975. *Astrophys. Lett.* 16:173
Swarup, G. 1975. *MNRAS* 172:501
Turland, B. D. 1975a. *MNRAS* 170:281
Turland, B. D. 1975b. *MNRAS* 172:181
Turland, B. D., Scheuer, P. A. G. 1976. *MNRAS* 176:421
Tyson, J. A., Crane, P., Saslaw, W. C. 1977. *Astron. Astrophys.* 59:L15
Valentijn, E. A. 1978. *Astron. Astrophys.* 68:449
Valentijn, E. A. 1979a. *Astron. Astrophys. Suppl.* 38:319
Valentijn, E. A. 1979b. *Astron. Astrophys.* 78:367
Valentijn, E. A., Perola, G. C. 1978. *Astron. Astrophys.* 63:29
Vallée, J. P., Kronberg, P. P. 1975. *Astron. Astrophys.* 43:233
Vallée, J. P., Wilson, A. S. 1976. *Nature* 259:451
Vallée, J. P., Wilson, A. S., van der Laan, H. 1979. *Astron. Astrophys.* 77:183
Valtonen, M. J. 1977. *Ap. J.* 213:356
Valtonen, M. J. 1979. *Ap. J. Lett.* 227:L79

van Breugel, W. J. M. 1980a. *Astron. Astrophys.* 81:265
van Breugel, W. J. M. 1980b. *Astron. Astrophys.* 81:275
van Breugel, W. J. M. 1980c. *Astron. Astrophys.* In press
van Breugel, W. J. M., Miley, G. K. 1977. *Nature* 265:315
van der Kruit, P. C., Allen, R. J. 1976. *Ann. Rev. Astron. Astrophys.* 14:417
van der Laan, H. 1963. *MNRAS* 126:535
van der Laan, H., Perola, G. C. 1969. *Astron. Astrophys.* 3:468
von Hoerner, S. 1964. *Ap. J.* 140:65
Waggett, P. C., Warner, P. J., Baldwin, J. E. 1977. *MNRAS* 181:465
Wehinger, P. A., Wyckoff, S. 1978. *MNRAS* 184:335
Weiler, K. W. 1973. *Astron. Astrophys.* 26:403
Weiler, K. W., Johnson, K. J. 1980. *MNRAS* 190:269
Wiita, P. J. 1978a. *Ap. J.* 221:41
Wiita, P. J. 1978b. *Ap. J.* 221:436
Wilkinson, P. N. 1972. *MNRAS* 160:305
Wilkinson, P. N. 1974. *Nature* 252:661
Willis, A. G. 1978. *Physica Scripta* 17:243
Willis, A. G., Strom, R. G. 1978. *Astron. Astrophys.* 62:375
Willis, A. G., Strom, R. G., Wilson, A. S. 1974. *Nature* 150:625
Willis, A. G., Wilson, A. S., Strom, R. G. 1978. *Astron. Astrophys.* 66:L1
Wilson, A. S., Vallée, J. P. 1977. *Astron. Astrophys.* 58:79
Yabushita, S. 1979. *MNRAS* 188:59
Yee, H. K. C., Oke, J. B. 1978. *Ap. J.* 226:753
Young, P. J., Westphal, J. A., Kristian, J., Wilson, C. P., Landauer, F. P. 1978. *Ap. J.* 221:721